END
DATE
FILMED
O 81
DTIC

LEVEL

ARACOR

AD A103900

AN INVESTIGATION OF IMPURITY REDISTRIBUTION
EFFECTS AND SOLUBILITY/DIFFUSIVITY OF Cr IN GaAs

INTERIM TECHNICAL REPORT

By

T. J. MAGEE

PREPARED FOR:

DEFENSE ADVANCED RESEARCH PROJECTS AGENCY
1400 WILSON BOULEVARD
ARLINGTON, VIRGINIA 22209

ATTENTION: MR. S. ROOSILD

MONITORED BY:

OFFICE OF NAVAL RESEARCH
DEPARTMENT OF THE NAVY
800 NORTH QUINCY STREET
ARLINGTON, VIRGINIA 22217

ADVANCED RESEARCH AND APPLICATIONS CORPORATION

81 9 08 99

REPORT DOCUMENTATION PAGE		READ INSTRUCTIONS BEFORE COMPLETING FORM
1. REPORT NUMBER	2. GOVT ACCESSION NO. AD-A103 900	3. RECIPIENT'S CATALOG NUMBER
4. TITLE (and Subtitle) AN INVESTIGATION OF REDISTRIBUTION EFFECTS AND SOLUBILITY/DIFFUSIVITY OF Cr in GaAs		5. TYPE OF REPORT & PERIOD COVERED Interim Report, 1 May 1980 — Nov. 1980
		6. PERFORMING ORG. REPORT NUMBER
7. AUTHOR(s) T.J. Magee, C. Leung, R. Ormond, R.A. Armistead, D. Stevenson*, C.A. Evans, Jr., D.S. Day† and M. Omura† *Stanford University †Avantek, Inc.		8. CONTRACT OR GRANT NUMBER(s) N00014-80-C-0482
9. PERFORMING ORGANIZATION NAME AND ADDRESS Advanced Research & Applications Corporation 1223 East Arques Ave., Sunnyvale, CA 94086		10. PROGRAM ELEMENT, PROJECT, TASK AREA & WORK UNIT NUMBERS PE 61101E Project OD10 Task NR 243-031
11. CONTROLLING OFFICE NAME AND ADDRESS Defense Advanced Research Projects Agency Materials Sciences Office 1400 Wilson Blvd., Arlington, VA 22209		12. REPORT DATE November 1980
		13. NUMBER OF PAGES 57
14. MONITORING AGENCY NAME & ADDRESS(if different from Controlling Office) Office of Naval Research Code 427, M. Yoder Arlington, Virginia 22217		15. SECURITY CLASS. (of this report) Unclassified
		15a. DECLASSIFICATION DOWNGRADING SCHEDULE

16. DISTRIBUTION STATEMENT (of this Report)

Approved for public release; distribution unlimited.

DTIC
ELECTE
SEP 8 1981

H

17. DISTRIBUTION STATEMENT (of the abstract entered in Block 20, if different from Report)

18. SUPPLEMENTARY NOTES

ONR Scientific Officer
Telephone: (202)696-4218

19. KEY WORDS (Continue on reverse side if necessary and identify by block number)

Gallium arsenide	Diffusion	Epitaxial layers
Defect gettering	Impurity effects	Reliability
Impurity gettering	electrical contacts	
Semiconductors	Annealing	
Field effect transistors	Implantation damage	

20. ABSTRACT (Continue on reverse side if necessary and identify by block number)

Experiments have begun on the investigation of the thermodynamics and phase equilibrium of the Ga-Cr-As system and the soulubility and diffusivity of Cr in GaAs under selected conditions of temperature and source composition. Allied experiments on the influence of defects in GaAs have shown that stable front surface Cr depletion channels can be formed in GaAs for retarding the outdiffusion of Cr. Investigations of the influence of non-stoichiometric regions introduced by implantation (as predicted by the →

DD FORM 1473
1 JAN 73

Christel-Gibbons model) on the redistribution of Cr after annealing have shown a definitive correlation between predicted damage zones and experimentally observed gettering regions.

The field enhanced diffusion of Cr into contact regions of GaAs-FETs under accelerated thermal-bias stress testing has now been shown to be correlated with the degradation of contacts during stress.

Separate experiments on CZ-Si containig oxygen have demonstrated that oxygen is extremely mobile in Si and can be gettered into damage regions at temperatures as low as 350°C.

Accession For

NTIS CRA&I
DTIC TAB
Unannounced
Justification

By
Distribution/
Availability Codes
Avail and/or
Dist   Special

A

CONTENTS

iii

FIGURES

TABLES

1. INTRODUCTION

1.1 BACKGROUND

Gallium arsenide (GaAs) device fabrication requires semi-insulating substrates. In order to achieve high resistivities in GaAs substrates, the effects of impurities and deep level traps within the material must be compensated. These impurities have been successfully compensated by Cr additions to achieve resistivities $\geq 10^7$ -cm in GaAs. However, recent investigations have shown that the behavior of Cr has not been properly understood and a number of problems occuring during GaAs device fabrication can be attributed, in part, to the anomalous redistribution of Cr both during and subsequent to thermal processing.

In 1978, experiments within the United Kingdom by Tuck et al. using radiotracers showed that Cr diffuses readily in GaAs at temperatures in the range 720°C to 750°C, resulting in outdiffusion from the substrate into epitaxial layers grown on semi-insulating wafers. Their data suggested the diffusion of Cr cannot be explained by a simple substitutional motion and rather, an interstitial mechanism must be employed.

During the same period, independent experiments in the United States by T.J. Magee et al. on optimized back-surface-damaged GaAs samples showed that Cr was mobile at 750°C and could rapidly gettered within damaged regions in the range 650°C to 750°C. Subsequent experiments showed that Cr could also be gettered by damage introduced in the GaAs during implantation of active impurities such as Se or S and that stresses introduced by the encapsulant at the interface would also getter Cr. These results partially explain the often observed existence of "dead" layers in ion-implanted (capped) samples after annealing.

Following these initial experiments, investigations by researchers at Hughes Research Laboratory, Rockwell International and Hewlett Packard have confirmed the redistribution behavior of Cr during thermal processing. However, detailed experiments to investigate the solid solubility of Cr in GaAs, to quantify diffusion constants and to determine the influence of lattice defects on diffusion have not as yet been performed. Equally lacking is information on the influence of other impurities such as C, O, and B (typically included in LEC material). Detailed analyses of the effect of dopants, such as Si, Sn, Se, S, or Te, on Cr diffusion have also not been performed, although preliminary experiments by our group on Sn-doped LPE layers and Si-doped VPE layers showed that the diffusion of Cr within the epitaxial layers is markedly altered.

Of additonal interest is the possible correlation between contact degradation and Cr diffusion during accelerated thermal stress-bias testing of devices. Initial research reported by ARACOR has shown that Cr redistributes and getters into contact regions during the alloying sequence. At that time, it was suggested that Cr redistribution was possibly responsible for long-term contact degradation during accelerated life testing. However, no experiments have been reported on the combined role of electric field and thermal stress on the redistribution of Cr and its effect of contact failure.

The objective of this program is to provide a detailed investigation of the role of defects and impurities in the GaAs lattice, with particular emphasis on the behavior of Chromium. The program includes a study of the thermo-dynamics and phase equilibrium of the Ga-Cr-As system; an investigation of the solubilities of Cr in GaAs under selected

2

conditions of temperature and source composition; and mea-
surements of the diffusivity if Cr in GaAs, with emphasis
on the diffusion of Cr in a concentration gradient. In
addition, the role of defects and resolvable complexes
will be investigated in relation to Cr-difffusion. The role
of defects, bias-voltage (field) and additional dopants will
also be investigated to determine the possible relationship
between Cr diffusion and electric field in relation to con-
tact degradation. This report summarizes briefly the data
obtained to date on this program.

1.2   SUMMARY OF RESULTS

During the first six months period of this program,
the following results have been obtained:

o   Investigation of front surface Cr depletion channels
    formed by B implantation into GaAs and subsequent
    annealing in arsine.

o   Investigation of electrical transport properties
    within Cr depletion channels in GaAs.

o   Preliminary investigations of the low temperature
    stress-bias degradation of ohmic contacts on GaAs
    FET devices.

o   Identification of field enhanced diffusion of Cr in
    GaAs.

o   Investigation of the Cr-Ga, As-Cr systems, DTA
    measurements and surface degradation studies in Cr-
    doped GaAs.

o   Initial evaluation of CdTe and HgCdTe substrates used in IR detector fabrication.

o   Initial experiments on the enhanced diffusion of oxygen in Si in the presence of microstructural damage.

1.3   PUBLICATIONS

The following publications were drawn in part or in total from this program of research:

a) "Incorporation of Boron During the Growth of GaAs Single Crystals," Applied Physics Letters 36, June 15, 1980 (pp.989-990).

b) "Low Temperature Gettering of Cr in GaAs," Applied Physics Letters 37, July 1, 1980 (pp.53-55).

c) "Annealing of Damage and Redistribution of Cr in Boron-Implanted, Si_3N_4 Capped GaAs," Applied Physics Letters 37, Sept. 1, 1980 (pp. 447-449).

d) "Low Temperature Redistribution of Cr in Boron-Implanted GaAs in the Absence of Encapsulant Stress," Applied Physics Letters 37, Oct. 1, 1980 (pp. 635-637).

1.4   TECHNICAL PRESENTATIONS

Process Technology for Direct Ion Implantation in Semi-Insulating III-V Materials-Workshop, University of California, Santa Cruz, August 12-13, 1980.

1) "Gettering of GaAs Wafers for Impurity and Defect Control"

2) "Front Surface Control of Cr Redistribution and Formation of Stable Cr Depletion Channels in GaAs"

2. FRONT SURFACE CONTROL OF Cr REDISTRIBUTION AND FORMATION OF STABLE Cr DEPLETION CHANNELS IN GaAs.

Over the past two years it has been demonstrated that Cr is rapidly redistributed in GaAs at temperatures in the range 300° to 1000°C, using established encapsulation procedures and capless techniques during annealing[1-8]. However, there have been no reported investigations on methods for controlling Cr redistribution at the surface or within ion implanted regions of GaAs.

In recent papers,[9,10] we discussed the development of Cr-depletion regions in B-implanted GaAs annealed in flowing H_2 both in the presence of an Si_3N_4 encapsulatant and in the absence of an encapsulating layer. This section presents correlated data from secondary ion mass spectrometry (SIMS), capacitance-voltage (C-V) and Hall effect measurements showing the formation, control and stability of Cr-depletion zones created in B-implanted GaAs after annealing in _arsine_ and the development of stable n-type conduction across the depletion channel.

Gallium arsenide wafers used in this study were of (100) orientation and grown by the Bridgman technique. Background Cr-doping levels were in the range, 4×10^{16} to 2×10^{17} atoms-cm^{-3}. After cleaning, the GaAs wafers were implanted with 100 keV B-ions to a dose of 5×10^{14} ions cm^{-2}. Annealing was done in a horizontal quartz reactor tube with a quartz wafer holder. A flowing gas mixture of Pd-diffused H_2 (400 cc/min.) and 5% AsH_3 in H_2 (20 cc/min.) was used for the required annealing temperatures ($T_A \leq 850°C$). For T_A = 900°C, the AsH_3/H_2 flow rate was increased to 30 cc/min. Under these conditions, a partial pressure of arsenic was produced in excess of the equilibrium partial pressure of arsenic at the GaAs surface[11] and was shown to be adequate for the range of annealing temperatures used in this study.

6

Carrier concentration profiles were obtained from differential capacitance-voltage (C-V) measurements using a Shandon Southern Impurity Profile Plotter and Hg probes for making contacts to the wafer. Hall effect/sheet resistivity measurements were made using the standard van der Pauw technique[12]. Carrier concentration depth profiles were obtained using acid layer removal and Hall effect measurements. Incremental layers were removed by immersing samples in an NH_4OH: H_2O_2: H_2O (2:1:100) solution, producing an etching rate of $\cong 30Å/sec$.

Samples for SIMS profiling analyses were prepared in the form of 5 mm squares. Both control (no implantation) and implanted samples subjected to similar annealing schedules were investigated to provide comparative information on Cr-redistribution. A Cameca IMS-3f ion microanalyzer with O_2 primary ion bombardment and positive secondary ion spectroscopy was used for impurity profiling. Atomic concentrations of Si, Cr, B and other impurities were calibrated using standards prepared by ion implantation into GaAs substrates.

Secondary ion mass spectrometry profiles of the Cr-impurity distribution within control (not implanted) wafers used in these experiments showed <u>no</u> significant surface redistribution of Cr after annealing in arsine at temperatures $\leq 850°C$. In Fig. 1 we show representative SIMS profiles obtained from separate samples of the B and Cr concentrations after B implantation and subsequent annealing in arsine for 1 hour at temperatures of 650°C, 750°C and 800°C. Also shown for reference are SIMS profiles of the Cr distributions in implanted (unannealed) and control (annealed, not implanted) samples. At temperatures <850°C, we observe no detectable diffusion of the implanted B, in agreement with earlier results.[9,10,13] In Figure 1a), after annealing at 650°C
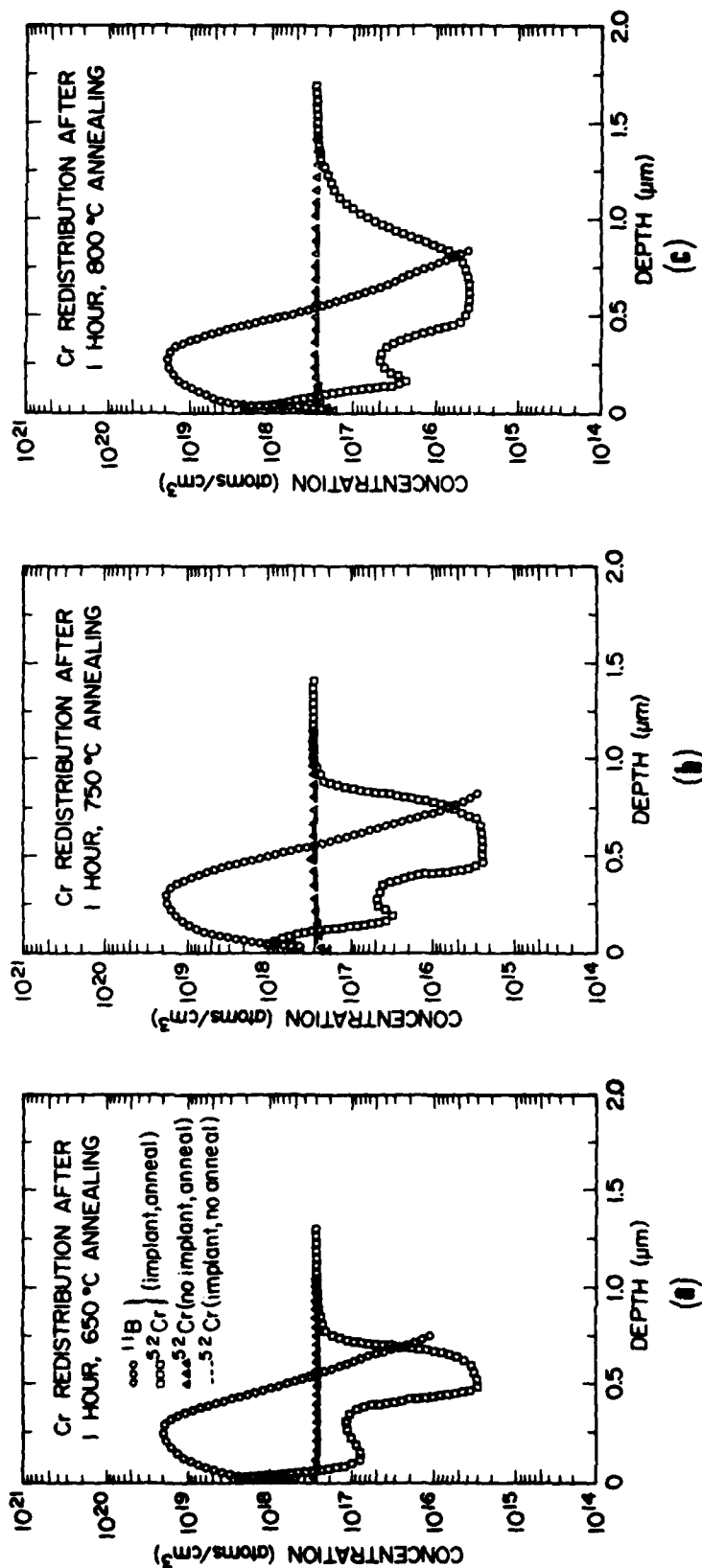
FIG. 1. SIMS PROFILES OF B AND Cr CONCENTRATIONS AFTER IMPLANTATION OF B AND SUBSEQUENT ANNEALING IN ARSINE AT VARIABLE TEMPERATURES FOR 1 HR; (a) 650°C; (b) 750°C; (c) 800°C. CHROMIUM CONCENTRATION PROFILES ARE ALSO SHOWN FOR REFERENCE IN IMPLANTED (UNANNEALED) AND ANNEALED (UNIMPLANTED) CONTROL SAMPLES.

we observe a rapid depletion and subsequent motion of Cr toward the surface, creating a zone of Cr depletion and a relatively sharp shoulder at $\simeq$ 0.75 μm. As the temperature is increased to 750°C (Figure 1b) the Cr depletion zone expands inwards forming a buried channel zone 0.5 μm in width. At the outer edge of the channel, gettered Cr is present within damage regions at R_p, the projected range. At 800°C, the amount of Cr gettered within damage at R_p is further decreased, accompanied by additonal motion of Cr toward the surface and an increase in the effective width of the depletion channel (Fig.1c).

The Cr redistribution shown in Figure 1 is in sharp contrast to the results observed with implants of heavier ions in GaAs after annealing at temperatures $\leq$850°C.[2,7,14] For temperatures > 850°C, we detected a breakdown of the channel region and an annihilation of effective pinning of Cr at the edge of the implanted B-distribution. The resulting Cr distribution (T_A> 850°C) is then similar to profiles observed in previous experiments[9,13] and is characterized by the presence of a long depletion tail extending to a depth of 2 μm. From these results we can conclude that the thermal stability limit for channel definiton and Cr control is reached at anneal temperatures of <850°C.

To further extend these results, we performed a similar set of experiments using samples containing a Cr background concentration of 4 x 10^{16} atoms cm^{-3}. In Fig. 2, we show the Cr redistribution profile obtained after implantation and annealing at 750°C. Of particular interest is the formation of a well-defined "square well" Cr depletion channel extending to a depth $\simeq$ 1 μm from the surface. These experiments were repeated on a number of samples and essentially identical Cr redistribution profiles obtained. In agreement with the previous data, we observed a (channel) thermal stability limit at 850°C.
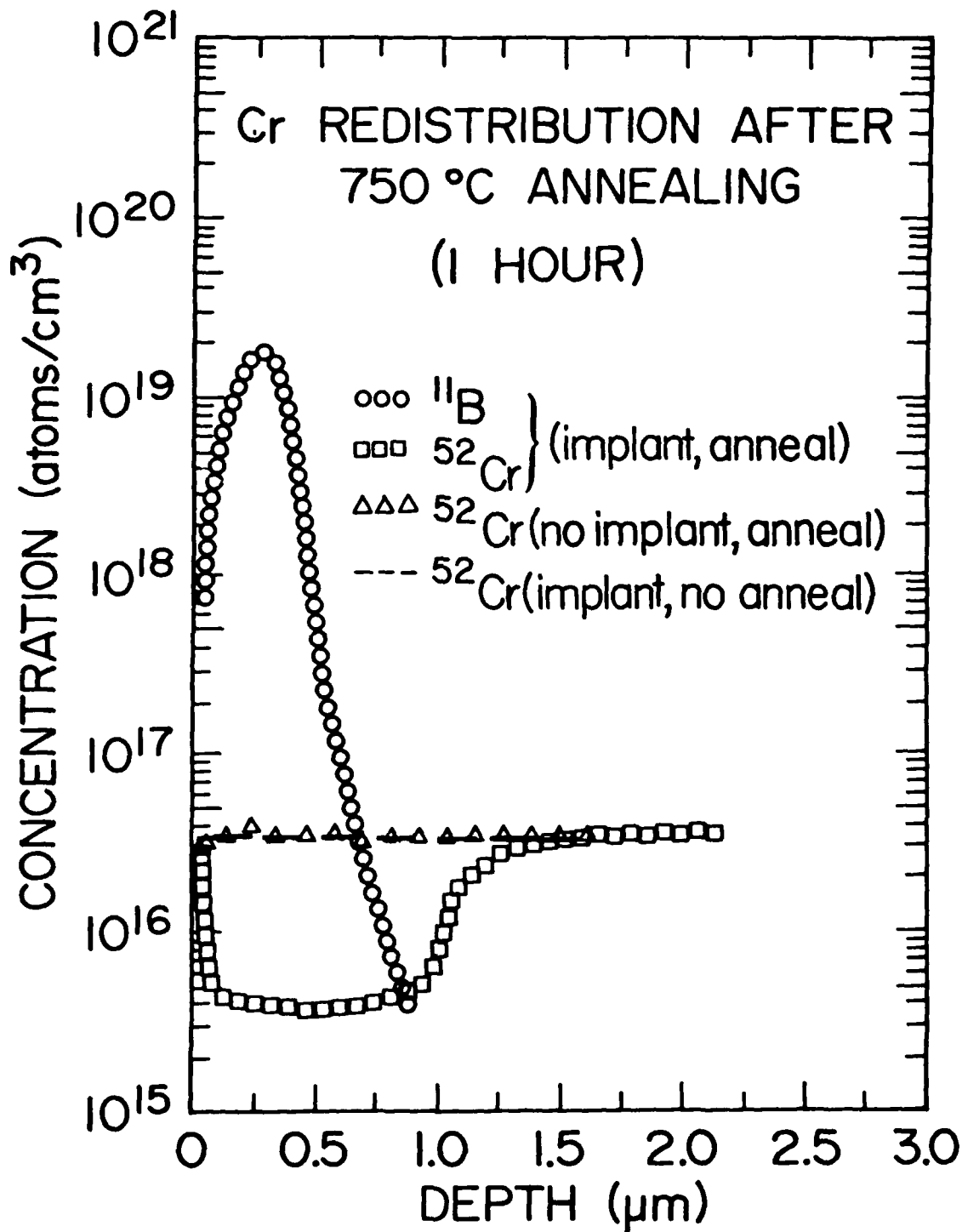
FIG. 2. SIMS PROFILES OF B AND Cr CONCENTRATIONS IN LOW (4×10^{16} ATOMS CM^{-3})-Cr-CONTENT GaAs WAFER AFTER B IMPLANTATION AND SUBSEQUENT ANNEALING IN ARSINE AT 750°C FOR 1 HR. ALSO SHOWN FOR REFERENCE ARE THE Cr CONCENTRATION PROFILES OBTAINED FROM IMPLANTED (UNAN-NEALED) AND ANNEALED (UNIMPLANTED) CONTROL SAMPLES.

To obtain information on possible conduction across the depletion channel in the presence of the implanted B distibution, we obtained C-V and Hall effect/stripping measurements on the implanted, annealed samples. In Fig.3, we show the electron concentrations and mobilities obtained at substrate temperatures of 77°K and 300°K for Hall effect measurements and 300°K for C-V measurements. Comparing the data of Figures 2 and 3, we observe that the maximum carrier concentration ($\approx 10^{16}$ cm^{-3}) extends to a depth of $\approx 0.8 \mu$m and is reduced rapidly at the edge of the Cr depletion channels. Since the background Si concentration determined from SIMS analyses was $\approx 1.6 \times 10^{16}$ atoms cm^{-3} and the net donor (N_D-N_A) atom concentration was $\approx 10^{16}$ atoms cm^{-3}, we can conclude that Si impurities in the GaAs are primarily responsible for conduction across the Cr-depletion zone.

Of interest is the fact that Hall mobilities were 5200 and 11600 cm^2/V-sec across the depletion channel at 300° and 77°K, respectively, in the presence of residual damage retained within the B-implantation region after annealing[9,10]. Since the peak B concentration was $\approx 10^{19}$ cm^{-3}, and $\approx 10^{16}$ carriers/cm^3 (background impurities) were detected across the B-implanted, Cr-depleted channel, it is apparent that boron does not significantly contribute to compensation in the GaAs lattice under the experimental conditions employed.

From the data obtained we can conclude that Cr-depleted channels can be created in GaAs using B-implantation and subsequent annealing in arsine. Pinning of Cr at the edge of the implanted B distribution occurs reproducibly and appears to be stable for anneal temperatures <850°C. Although the present experimental data do not permit an exact description of the depletion and pinning mechanisms, we can speculate that the diffusion of Cr within the implanted region is

11
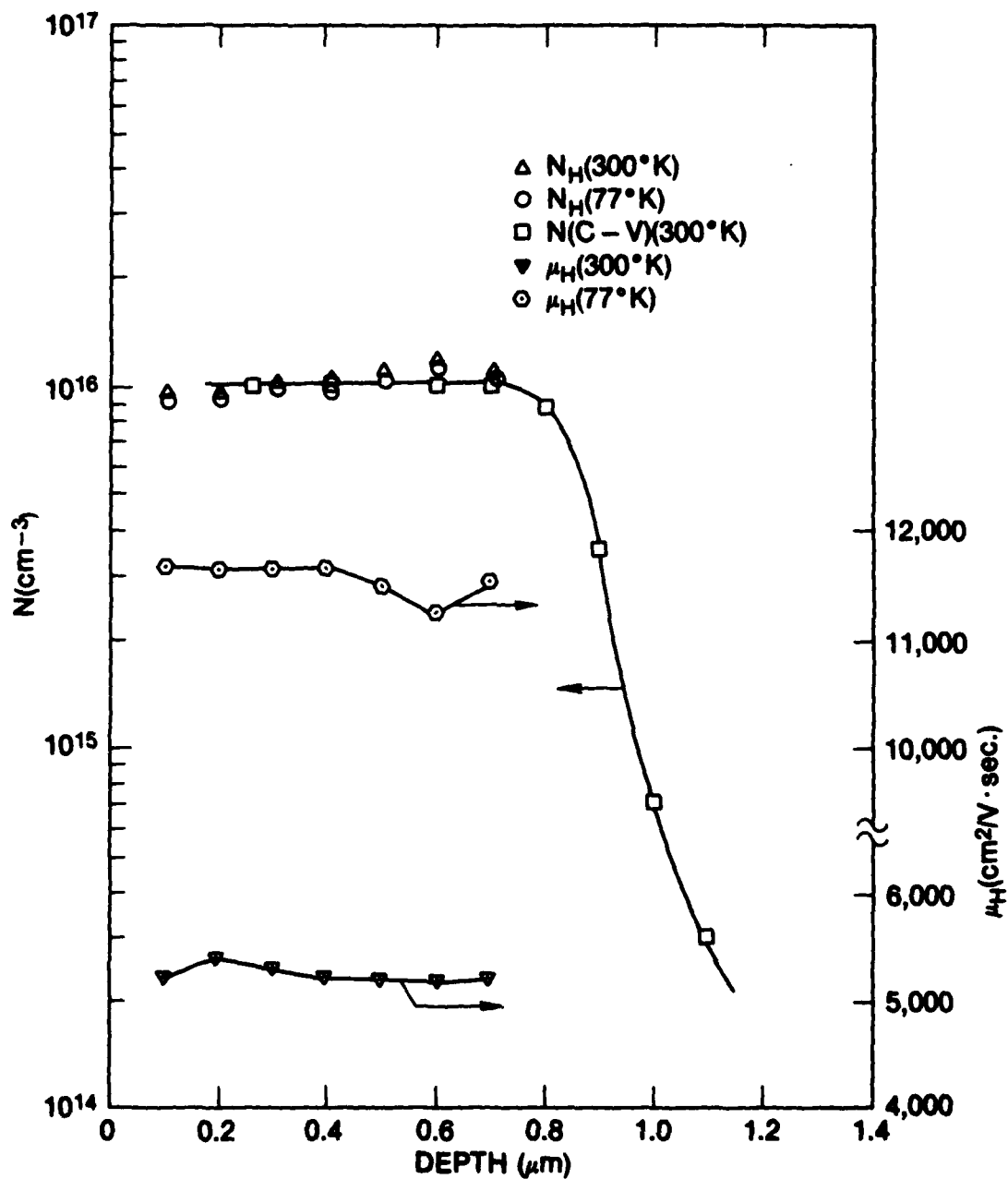
FIG. 3. ELECTRICAL PROFILES OBTAINED FROM C-V AND HALL-EFFECT/STRIPPING
MEASUREMENTS AT SUBSTRATE TEMPERATURES OF 77 AND 300K. ELECTRON
CONCENTRATIONS AND HALL MOBILITIES ARE PLOTTED AS A FUNCTION OF
DEPTH FROM THE SURFACE OF THE GaAs.

enhanced in the presence of implant damage and the redistribution of Cr correlated with the annealing of microstructural defects[9]. As the anneal temperature is increased above 500°C, Cr outdiffuses readily to the surface, creating a well defined channel and abrupt shoulder at the two edges of the boron distribution. In the presence of an implanted B impurity gradient, diffusion within the depletion channel is possibly retarded at these temperatures because of changes in the Cr diffusion coefficient. If indeed valid, this would explain the creation of the sharply defined shoulder in the Cr-distribution profile, but additional experiments are needed to provide definitive information.

It is conceivable that the observed phenomena may be useful for device applications, particularly for charged coupled devices, where a sharp depletion shoulder on the Cr distribution would be desirable.[15] Activation of secondary ion implanted impurities within the depletion channel should also be possible; however, it is felt that the boron dose level must be reduced to permit activation of ion implants ($\leqslant 10^{17} cm^{-3}$) used in device fabrication. Experiments are continuing and the results will be reported at a later date.

3. CHROMIUM REDISTRIBUTION AND STOICHIOMETRY DISTURBANCES IN ION IMPLANTED GaAs

In earlier papers we have shown that Cr is redistributed rapidly at temperatures of 400° to 500° in B-implanted GaAs in the absence of an encapsulating layer. Of particular interest in these studies is the fact that initial Cr depletion and gettering does not occur at depths equal to the projected range, Rp, where the maximum concentration of implant damage would be expected, but at depths exceeding Rp.

In recent studies, Christel and Gibbons have shown that ion implantation into compound semiconductors produces not only a characteristic damage region, but a non-stoichiometric distribution of the host atoms. Because of the differing masses of the Ga and As, the collision cross section, maximum energy transfer and recoil range distribution for each of the elements will be different, producing a varying Ga/As ratio as a function of depth into the sample, suggesting the possibility of interstitial concentrations at depths exceeding Rp.

In Fig. 4, we show the calculated profiles (after Christel and Gibbons) for an implanted B-distribution (50keV, $10^{15}/cm^2$) with the Ga-As vacancy concentration profiles and net Ga-As displacement plotted as a function of depth. It is of interest to note that the interstitial concentration profiles (net Ga-As displacements) occur at depths exceeding R_p and stoichiometric imbalance is produced at varying depths from the surface.

To further investigate the possible correlation between these predicted stoichiometric disturbances and Cr redistribution, we implanted B at energies of 50, 100 and 300 keV into Bridgman grown GaAs samples (in separate experiments)
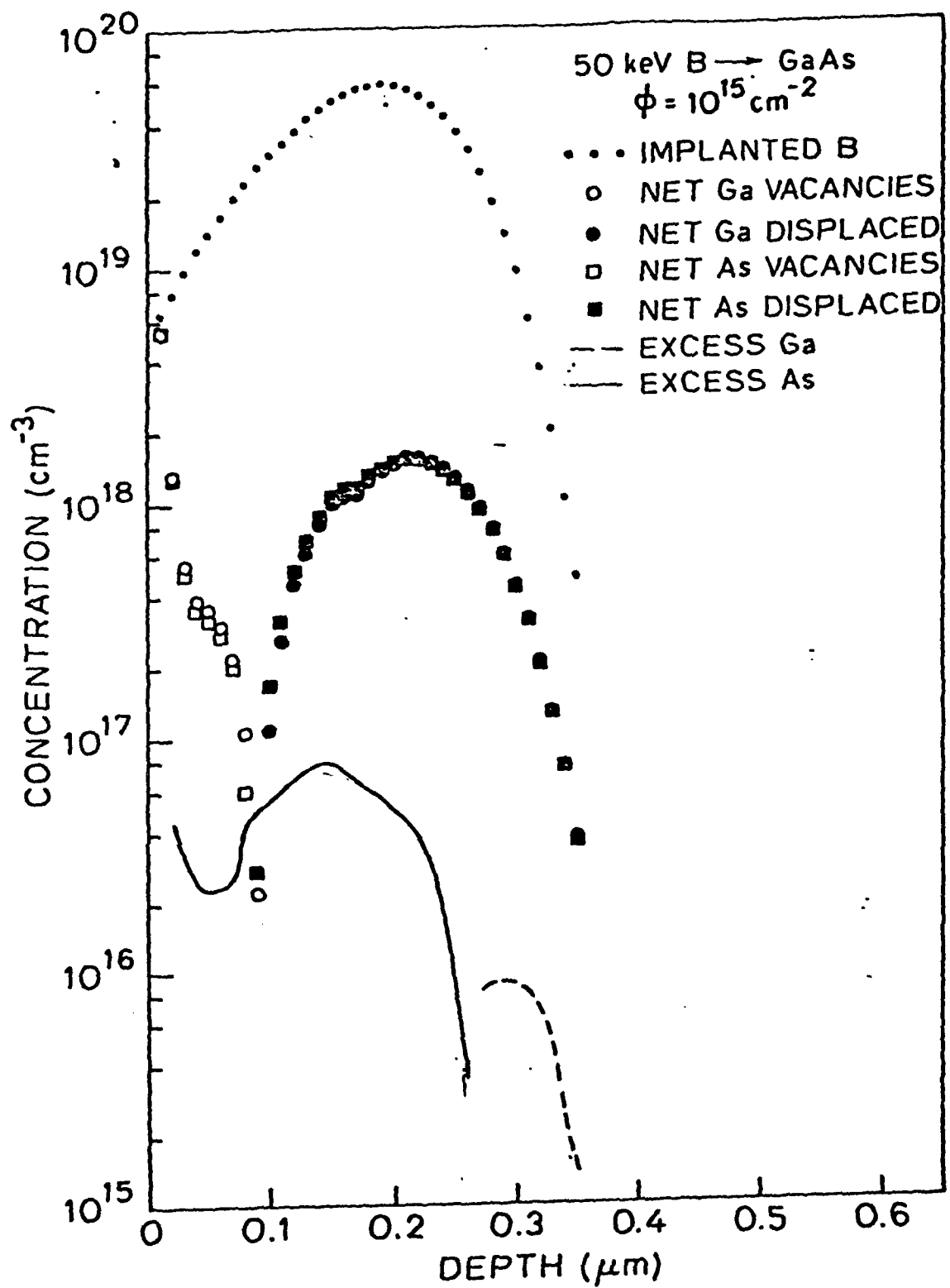
FIG. 4. NET Ga/As VACANCIES AND NET Ga/As DISPLACED FOR 50KeV B-IMPLANT INTO GaAs

to total doses of 10^{15}ions/cm^2. In Fig. 5 we show the Cr redistribution profiles obtained on 50 keV B-implanted (10^{15}/cm^2) GaAs samples subsequent to annealing (capless) in flowing H$_2$ at 500°C for 1 hr. Also shown for reference are the Christel-Gibbons calculated Ga-As vacancy and interstitial profiles after implantation. It can be observed that initial depletion and gettering of Cr occurs approximately at the edge and peak of the calculated interstitial profile, respectively. Under these annealing conditions and in the absence of an encapsulating layer, near-surface redistribution of Cr is essentially absent, as indicated in the figure.

Correlated TEM data obtained on the implanted annealed samples show a distribution of dislocation loops within the peak region of the predicted interstitial concentration and into the damage region at Rp. From this data, we can conclude that the interstitials produced during implantation are clustered (after annealing) in the form of observable dislocation loops. Gettering of Cr occurs within this zone in the presence of the interstitial clusters. Interaction and pinning of Cr at the edge of dislocation loops has been discussed in a number of earlier papers, although such discussions have been limited to the gettering of Cr by residual structure within damage zones at Rp.

To extend these results, we also performed a series of tests on samples implanted at 100 and 300 keV to similar dose levels and annealed under the same conditions. Preliminary data show that a similar pattern of Cr distribution and gettering is observed, with interstitial loop concentrations present at depths > Rp.

16
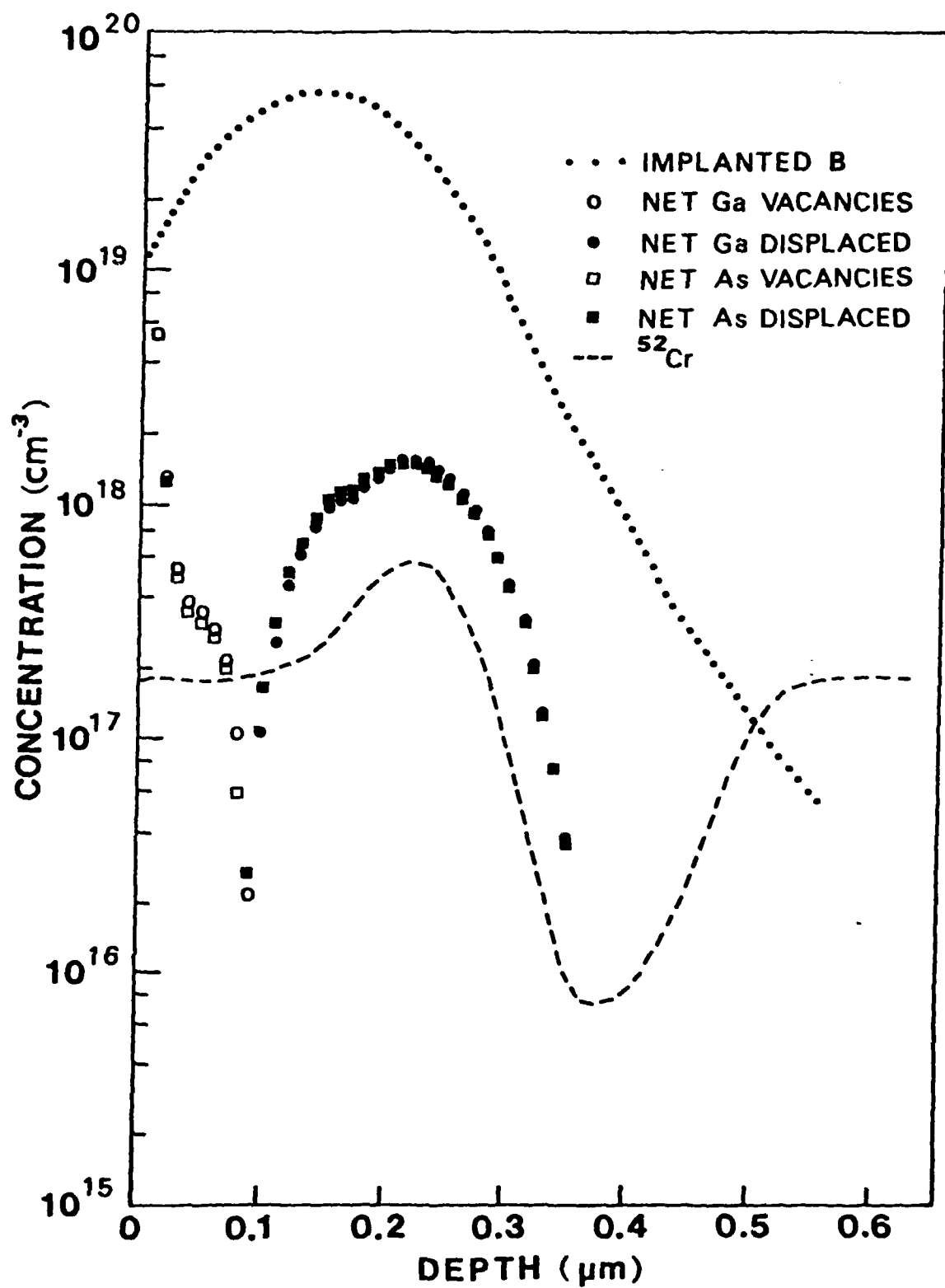
FIG. 5.   NET Ga/As VACANCIES, NET Ga/As DISPLACED AND Cr   REDISTRIBUTION
          PROFILE IN 500°C, ANNEALED, 50 KeV B-IMPLANTED GaAs SAMPLE.

Based on the current experiments, we observe a definite correlation between the Christel-Gibbons model and the observed Cr redistribution. Further work is required, however, to assess the influences of predicted stoichiometric disturbances on Cr redistribution in samples implanted with heavier ions (S,Se,Si) to doses known to produce an amorphous layer.

4. FIELD ENHANCED DIFFUSION OF Cr AND CONTACT DEGRADATION IN GaAs FETs

The problem of contact degradation in GaAs FETs has been an area of concern to device manufacturers for the past 10 years. Although numerous investigations have attempted to improve contact alloying procedures, there have been no definitive studies identifying mechanisms responsible for contact failure under thermal-bias stress testing.

Recently, we reported that simple short term alloying of Au contacts on substrates or LPE layers on S.I. substrates produced rapid redistribution and gettering of Cr into damage regions created by the low temperature alloying process. At that time, we suggested that accelerated motion of Cr into alloy zones and diffusion of Cr into interfacial regions might possibly be related to the observed contact failure during thermal-bias stress tests.

To further investigate this problem, GaAs FETs were fabricated by Avantek Inc. using conventional Au-Ge/refractory metal contact alloying on VPE (buffer/active) layers grown on S.I. substrates (Cr-doped).

In Fig. 6 we show an optical micrograph of the FET structure used in these experiments. To provide a systematic evaluation, we devised a series of test configurations for both electrical and impurity profiling tests. Figure 7 shows a matrix description of the tests conducted. The objective of the thermal-stress-bias tests was to determine the relative change in Rs and Rd as a function of stress time and to determine if the previously reported results of selective drain degradation could be related to the motion of Cr in the presence of an electric field.
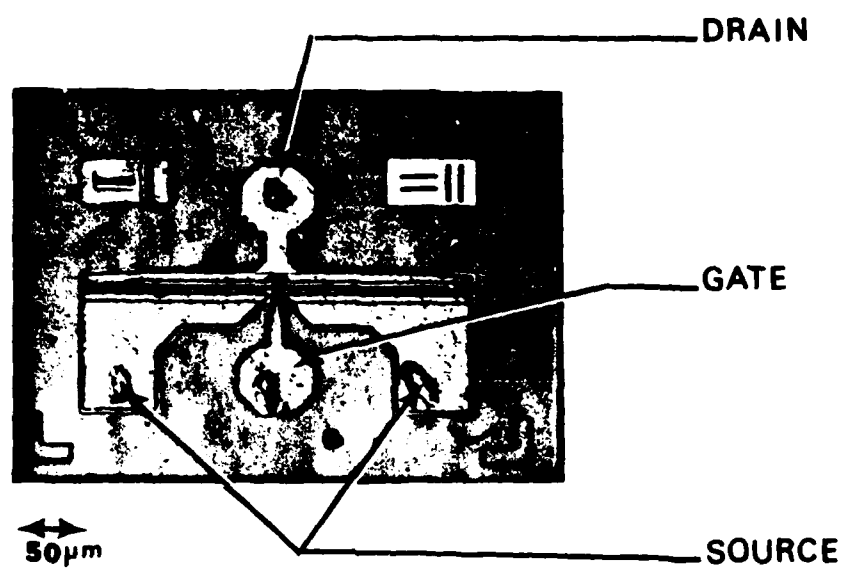
FIG. 6. OPTICAL MICROGRAPH OF FET TEST STRUCTURE.

TEST MATRIX
& STRESS CONDITION
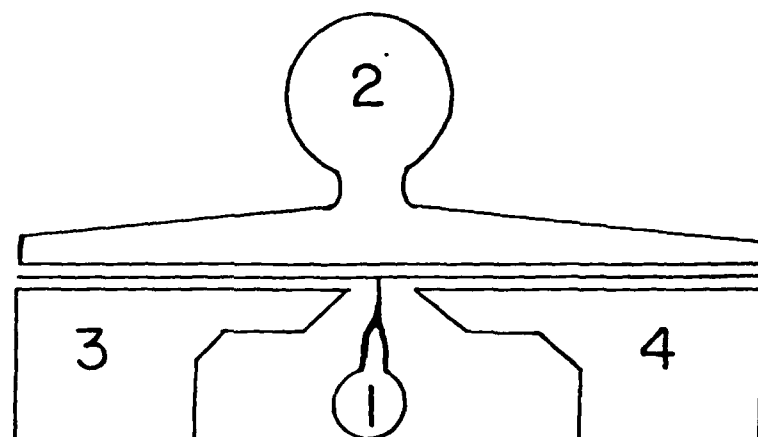
	Drain	Source	Gate	Not connected
Standard	2	3, 4	1	NA
Case 1	3, 4	2	1	NA
Case 2	4	2	1	3

	$V_{ds}(V)$	$I_{ds}(mA)$
Standard A	3	10
Standard B	3	20
Standard C	5	10
Standard D	0	0
Case 1	3	10
Case 2	3	5

FIG. 7. TEST MATRIX FOR ACCELERATED STRESS-BIAS TESTS.

G-064

In Fig. 8, we show Cr concentration profiles in depth obtained within the drain contact region after alloying and after subsequent annealing at 270°C for 161 hrs. (no bias). In both the source and drain contact regions, we observe a significant gettering of Cr, both within alloy damage regions and slightly deeper into the VPE layer. This motion and gettering of Cr into near-surface regions occurs <u>during</u> contact alloying, in agreement with our earlier reported results on modeled contact structures. After annealing for 161 hrs. at 270°C following contact alloying, we observe no significant alteration in the concentration of Cr within the near surface regions. These results are consistent for both drain and source contacts, showing that no further redistribution of Cr occurs (after alloying) during extended low temperature annealing.

In Fig. 9, we show the Cr redistribution profiles obtained from an FEI within source and drain contacts after thermal bias stress (5V,10mA;270°C). After 116 hrs. of stress, we detect essentially identical distributions of Cr under the source contact as observed after alloying, in agreement with the data shown in Fig. 1. Under the drain contact, however, we observe significant diffusion and pileup of Cr at the metallization/GaAs interface. Increased motion and pileup of Cr occurs as a function of increasing stress time.

The results show that Cr diffuses under the drain region producing a region ($1000\overset{\circ}{A}$ to $2000\overset{\circ}{A}$ thick) near the surface containing high concentrations of Cr ($>10^{20}/cm^3$). In the source region, there is no pronounced diffusion of Cr to the surface and the Cr concentration remains the same as observed after contact alloying.
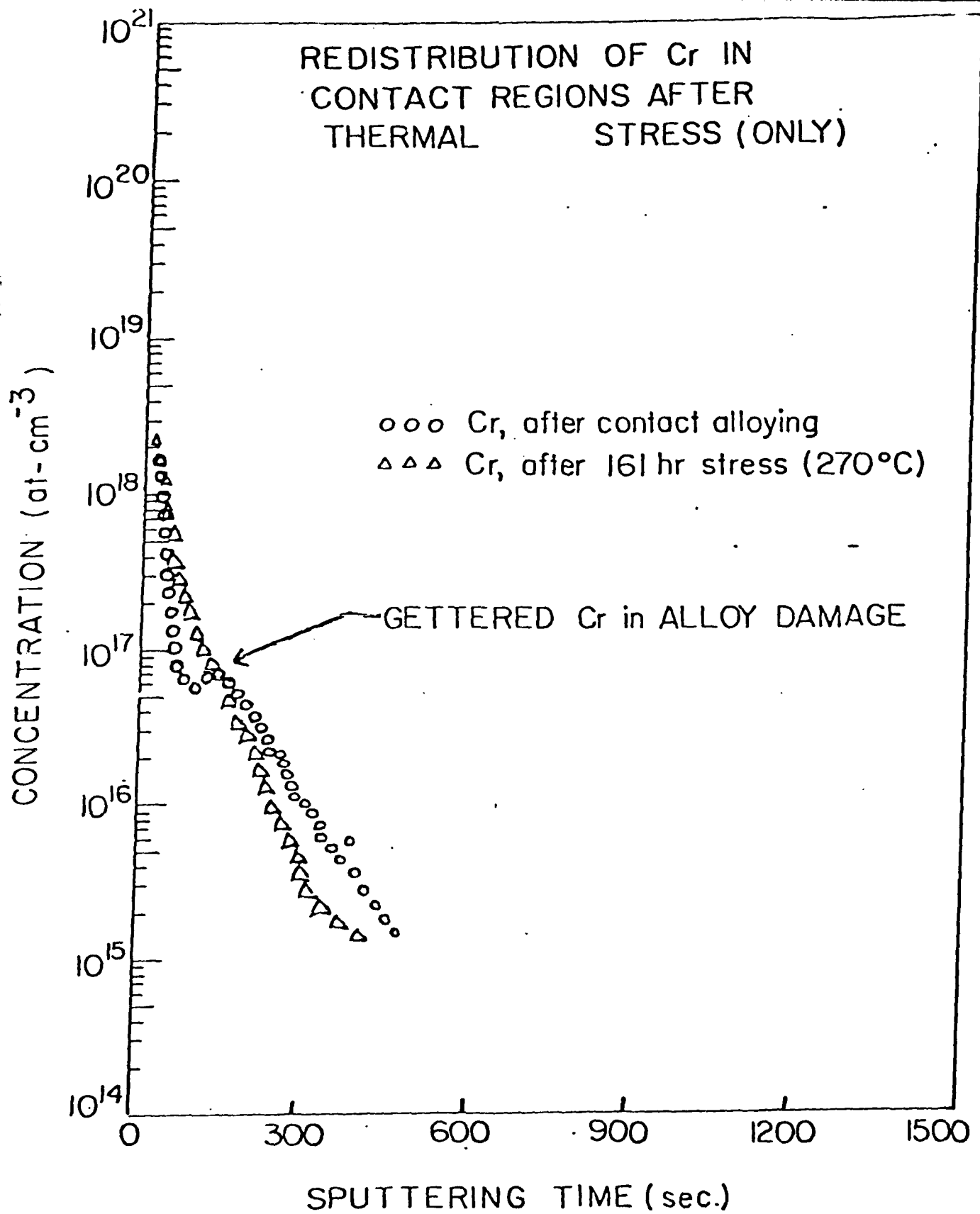
FIG. 8. CHROMIUM REDISTRIBUTION PROFILES IN DEVICES SUBJECTED TO THERMAL STRESS (ONLY)
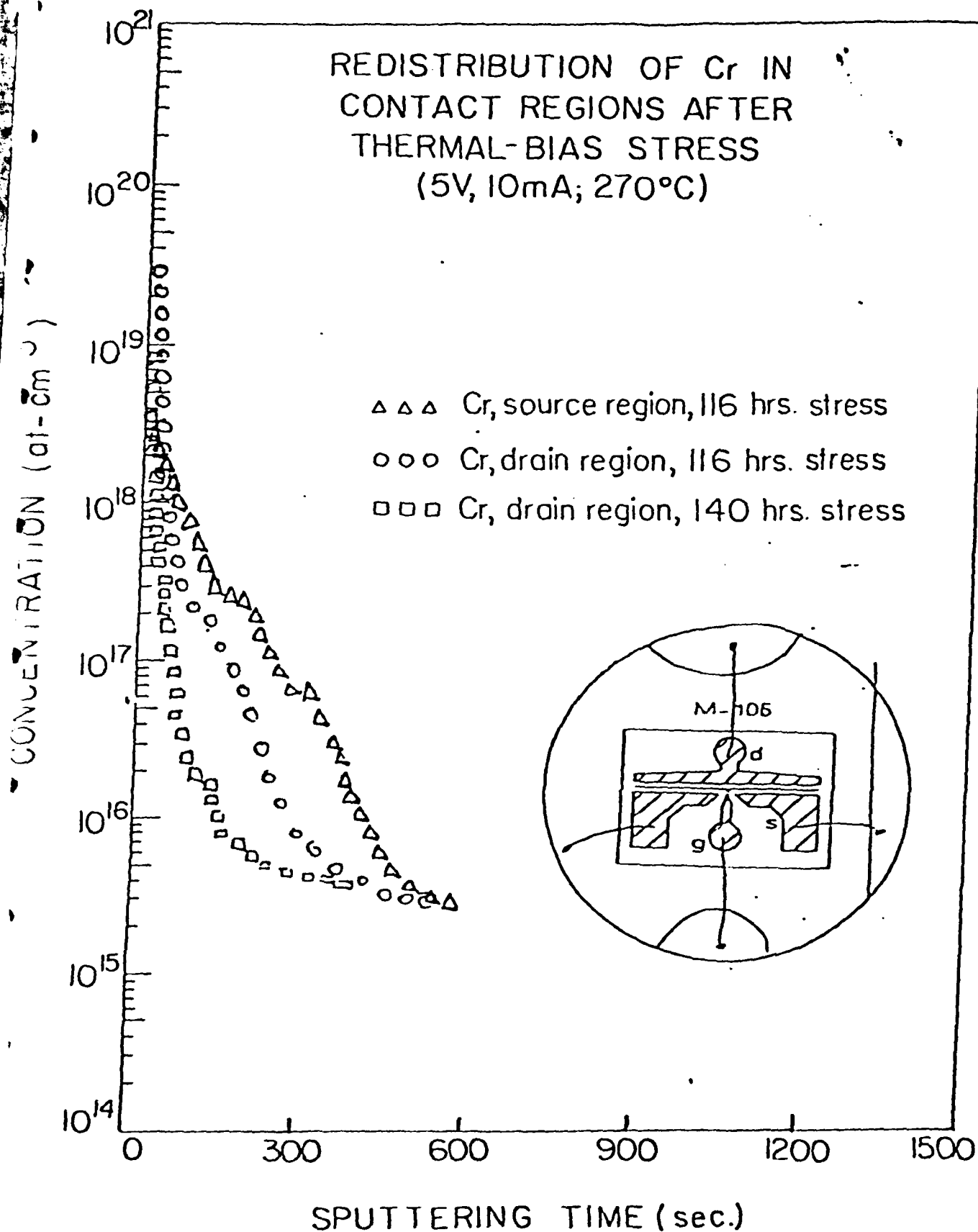
23

FIG. 9. CHROMIUM REDISTRIBUTION PROFILES IN CONTACT REGIONS AFTER THERMAL-BIAS STRESS (5V, 10mA; 270°C) FOR VARIABLE PERIODS.

Figure 10, shows Cr redistribution profile under source and drain contacts after thermal-bias stress under reduced voltage-bias conditions (3V,20mA;270°C). We observe a similar pattern of diffusion under the drain contact, while the source region shows no prominent redistribution of Cr after stress testing. Of interest, however, is the fact that the displacement of the Cr diffusion front is reduced relative to results obtained at 5V for comparable stress periods. These results suggest that the diffusion and pileup of Cr at the surface is directly proportional to the magnitude of the applied voltage.

To further evaluate the effect of voltage bias on Cr diffusion we performed a similar series of experiments in which the voltage remained constant and the input current was varied in a second series of tests, the current was held constant and the voltage increased in separate experiments. The results showed that the amount of Cr diffusing to the surface under the drain contact was influenced predominantly by the magnitude of the applied voltage. Changes in current did not produce any significant alterations in the pattern of Cr motion, verifying that voltage is the important factor in the enhanced diffusion of Cr.

To provide further confirmation of the field-enhanced diffusion of Cr in contact regions we reversed the polarity on source and drain regions (Fig. 11) and performed additional stress tests. (In the figure we have labeled source and drain regions in their normal configurations). The results show in dramatic fashion the polarity dependent diffusion effect, where the Cr pileup now occurs within the (initial) source region. Also shown for reference is the Cr redistribution on the unbiased (control) contact. It can be observed that no Cr redistribution can be detected and the observed profile is essentially identical to that obtained immediately after alloying.
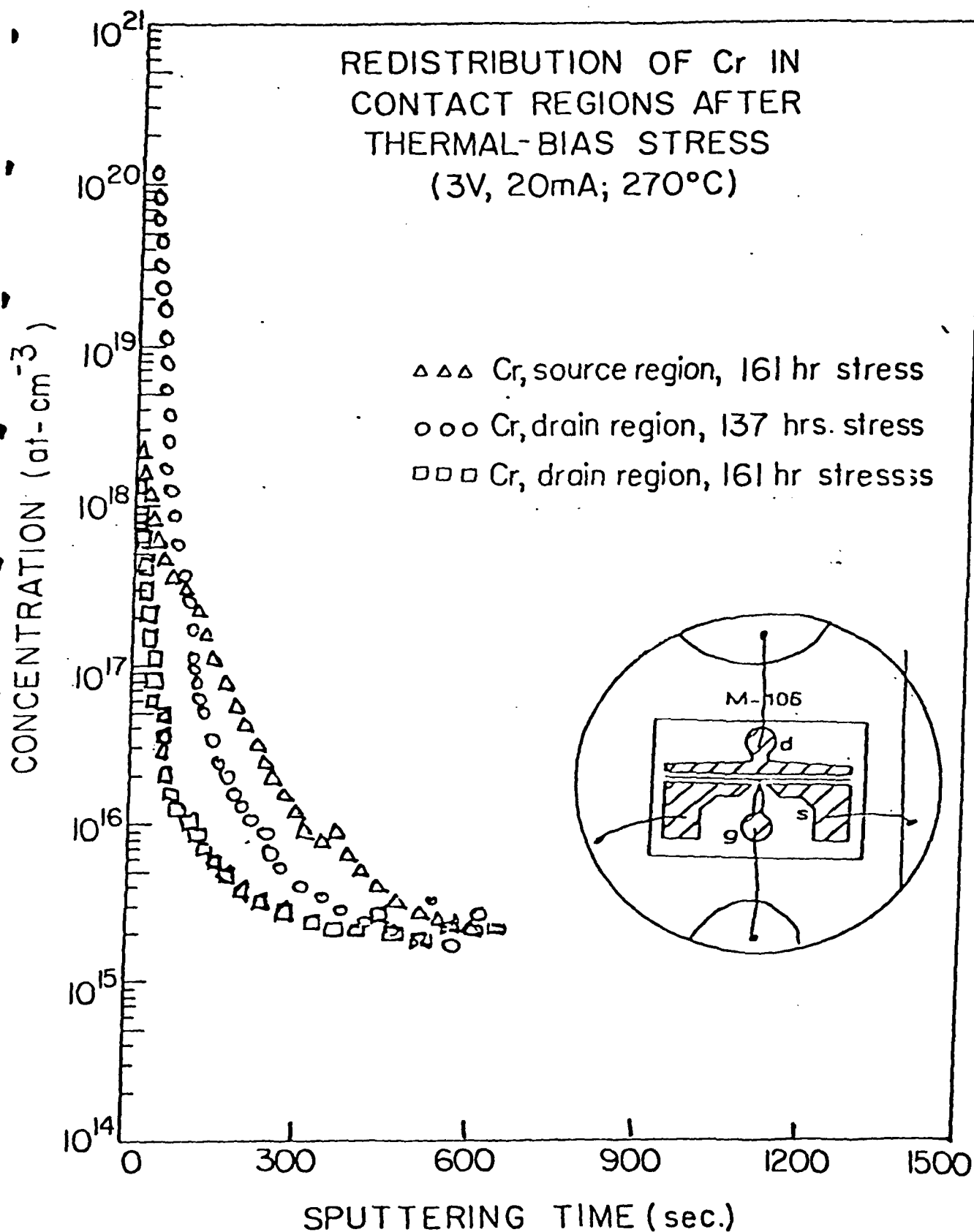
25

FIG. 10. CHROMIUM REDISTRIBUTION PROFILES IN CONTACT REGIONS AFTER THERMAL-BIAS STRESS (3V, 20mA; 270°C) FOR VARIABLE PERIODS.
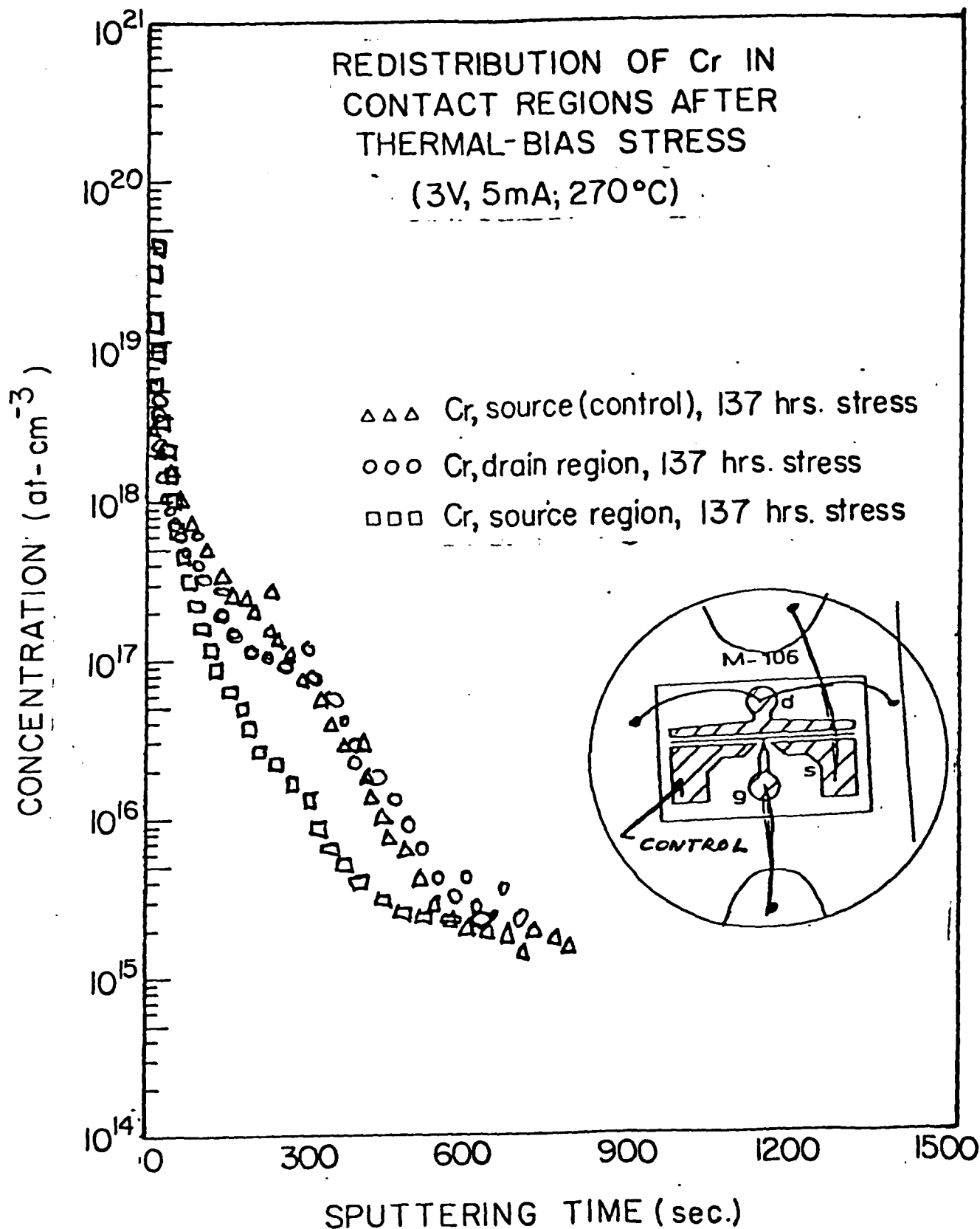
26

FIG. 11. CHROMIUM REDISTRIBUTION PROFILES IN CONTACT REGIONS AFTER THERMAL-BIAS STRESS (3V, 5mA; 270°C) FOR VARIABLE PERIODS

27

In Tables 1 and 2, we show representative data obtained on FETs subjected to stress-bias tests for varying times at 270°C. Also included for reference are average R_d and R_s values for devices subjected to thermal stress (only) at 300°C for 617 hrs. Devices subjected to thermal stress alone show no significant differences in R_d and R_s values after annealing. In comparison, under thermal-bias stress at 270°C, when $V_{ds} = 5V$ and $I_{ds} = 10mA$, (Table 1) we observe that the value of $R_d > R_s$ upon completion of the tests. Similarly, in Table 2 for $V_{ds} = 3V$, $I_{ds} = 10mA$, we observe a similar pattern of contact degradation, in which the drain resistance always exceeds the source resistance after thermal-bias stress. In an extended series of tests, we have shown that $(R_d/R_s - 1)$ scales both as a function of increasing stress duration and V_{ds}.

From the data obtained, we can conclude that the failure mode in the GaAs FETs can be explained by the field-enhanced migration of Cr into the drain region, resulting in an increase in R_d relative to R_s upon extended stress testing. This failure mechanism has been shown to be applicable to all devices tested and seems to explain all the other GaAs FET long term failure modes reported by other workers.

The present results indicate that failure will occur even at Cr concentrations as low as $10^{15}/cm^3$. Additional tests are currently required to obtain comparative data on ion implanted source and drain regions within LEC material of varying Cr concentration. It would also be of interest to develop techniques for controlling the field-enhanced diffusion of both oxygen and chromium in GaAs-based device structures.

3V- 10mA 270°C

I_{dss} (mA)					R_s / R_d		$R_d/R_s - 1.00$ (%) $t = t_1$
t = 0	50 hr.	137	161	△	t_0	t_1	
42	34			8	5.4/5.0	6.0/6.8	
42	36			6	5.3/4.6	6.4/6.4	6.5
44	35			9	5.1/5.1	6.0/6.4	
44		28		16	5.0/5.0	6.5/7.4	
41		16		25	4.8/5.0	6.4/7.4	17.3
48		24		24	5.0/5.0	6.2/7.6	
43			14	29	5.0/4.9	N A	
48			28	20	5.5/4.8	N A	
40			17	23	5.0/5.0	N A	

TABLE I.   DEVICE DATA (3V, 10mA; 270°C)

5V - 10mA   270°C

I_{dss} (mA)					Rs / Rd		$R_d/-1.00 / R_{s(t=t_1)}$ (%)
t = 0	46(hrs.)	116	140	Δ	t_0	t_1	
44		16		28/64	4.5/6.0	6.2/10	
44		19		25/57	5.2/5.0	6.2/8.4	
47	32			15/32	5.1/5.0	6.4/5.8	
32			6	26/81	5.8/5.5	NA	AV.=31.5
40	27			13/48	5.2/5.6	6.0/7.2	
43			8	35/81	5.0/5.5	NA	
t=0		137	161				
no bias 26		16	-	10/38	6.6/6.2	7.4/7.6	
42		30	-	12/29	5/5.2	7.4/6.2	

Previous   Device   Runs

t=0	t=617 hr.	T(°C)	Vds	Ids
R_s AV. 4.6	6.8	300	0	0
R_d AV. 4.0	6.7			
t=0	t = 193 hr.	T(°C)	Vds	Ids
R_s AV. 5.4	7.1	270	3	10
R_d AV. 4.9	12.3			

TABLE II. DEVICE DATA: BIASED AND UNBIASED, Ts = 270°C; Ts = 300°C

5. SOLUBILITY AND DIFFUSIVITY OF Cr IN GaAs

Semi-insulating wafers of Cr-doped GaAs are used extensively as substrates for the growth of active layers of GaAs by liquid or vapor techniques. The presence of Cr is believed to introduce deep levels in the band-gap which compensate residual impurities, leading to the semi-insulating properties.

In spite of the importance of this topic, relatively little work has been devoted to diffusion and solubility of Cr in GaAs. Two papers by Tuck and co-workers, however, report the results of studies devoted exclusively to the diffusion of Cr in GaAs, using radio-tracer techniques. Two major conclusions were found: diffusion profiles may not be represented by a simple error function solution, and diffusion coefficients are suprisingly large. The results indicate that Cr diffusion in GaAs may be a complicated process, perhaps with both interstitial and substitutional species playing a significant role.

To address these areas, a study of the solubility and diffusivity of Cr in GaAs in experimental systems, in which both diffusion sources and diffusion hosts are well characterized, was initiated. A major consideration is the proper definition of the phase relations in the Ga-As-Cr system and the relationship to diffusion sources of Cr in GaAs. The following three areas are emphasized in the study: phase relations in the Ga-As-Cr system, (with particular reference to establishing regions of co-existence of three phases); determination of the solubility of Cr in GaAs as a function of Cr source and the state of the GaAs host (eg. solute concentration and defect structure); and the diffusion of Cr in GaAs in a Cr concentration gradient, (with particular attention to careful definition of both to diffusion source and the GaAs host).

31

Possible isothermal ternary sections can be predicted
if three binary temperature-composition phase diagrams are
known. Our approach is to establish, to the best of our abi-
lity based on previous work and our own work the respective
binary systems. With this information, we can predict a few
possible isothermal ternary sections. We then wish to estab-
lish which of these possibilities is correct by performing
phase studies for a relatively few compositions. (The actual
type of ternary section will depend on which binary compounds
are the dominent ones.)

Once the general pattern of the ternary section is estab-
lished, the overall composition of three phase regions will
be established. Both defferential thermal analysis (DTA) and
X-ray diffraction (XRD) techniques will be used in this study.
We have carefully studied the original articles describing the
Ga-As, Ga-Cr and Cr-As systems. The first two systems have
been studied rather extensively, however, there are regions in
the Cr-As system, particularly at higher As compositions, that
are not reliably known.

To confirm previous work in the Ga-Cr system, we performed
DTA on 68.83 a/o Ga - balance Cr and obtained a liquidus tem-
perature within 4°C of that previously reported. We then de-
voted our efforts to the As-Cr system.

Because of its toxicity and high vapor pressure, As re-
quires particular care in handling. Rather than mixing dif-
ferent ratios of elemental As and Cr to perform DTA measure-
ments, we chose a different approach: the formation of the
compound CrAs at lower temperatures (500°C) by a long anneal,
and then the addition of either As or Cr to this compound to
obtain the desired compositions. Since CrAs has a much lower
vapor pressure than elemental As, the risk of a violent explo-
sion during DTA is reduced using this technique. A mixture of

32

30 gm As and /Cr in a 50-50 atomic ratio was sealed in a quartz ampule and heated to 500°C. However, after one day at this temperature, a small crack formed in the ampule, and fumes were escaping. Some compound formation was evident in the ampule, and this material was examined using an X-ray diffractometer. Diffraction peaks were found corresponding to both CrAs and Cr_4As_3, indicating that this material was this two-phase region. This is reasonable, since one would expect selective loss of As because of its higher vapor pressure. Several anomolous peaks also appeared in the diffraction pattern which cannot be indexed using existing information. Because of the difficulty in CrAs synthesis and because it is commercially available, we have purchased CrAs powder. We are using this to prepare Cr-As compositions for DTA as well as for Cr sources in solubility and diffusivity studies.

We were aware of potentially troublesome behavior during diffusion annealing due to the development of uneven surfaces on previously polished GaAs. Certainly, the selective vaporization of As at sufficiently high temperatures is to be expected in inert gas and vacuum environments. These problems are often described in the literature; however, there appears to be conflicting information. Malbon et al. for example, report that degradation occurs after a 20-minute anneal at 800°C in argon and that the degradation may be prevented by a suitable addition of As to the vapor ambient. Tuck et al. however, do not mention this problem, even for annealing as high as 1000°C without the intentional addition of excess As. This seems unusual since in the annealing of device structures, silicon nitride or silicon dioxide (or a combination) is customarily used to prevent surface degradation. This method (silicon nitride encapsulation) is not desirable for most diffusion studies, however, because it does not allow for well defined external sources of Cr or As.

To study surface decomposition of GaAs wafers under various conditions, several experiments were performed consisting of annealing polished GaAs wafers under well defined conditions and subsequent examination using interference contrast optical microscopy (100-1000X). Si-doped GaAs wafers were sealed in evacuated ampules with no source and annealed at 800°C, 900°C, 1000°C, and 1100°C for two hours each. Each sample was examined for surface degradation; degradation was observed in the samples at 1000°C and 1100°C, whereas the surface appeared unchanged at temperatures under 1000°C. Following these runs, elemental As powder was placed as a source in the sealed ampuled with the GaAs wafers. When the source was reduced to 0.38 atm in a second ampule at 1000°C, it is also showed strong degradation.

Initial diffusion experiments of Cr into GaAs were performed to 1) study effects on surface degradation, 2) compare Cr concentration profiles with previous experimen s, and 3) study the effects of using various Cr sources.

In all experiments, the undoped GaAs wafer (1cm x 1cm) was encapsulated in an evacuated quartz ampule, with the source material contained in a bulb at the end of the ampule (3cm from wafer). The ampules were placed in the flat zone of the furnace for the desiganted time and temperature, and then quenched.

For the first experiment, two GaAs wafers were annealed for two hours with a Cr (solid pellet) source, one at 900°C ($P_{Cr}=10^{-16}$atm) and the other at 1100°C ($P_{Cr}= 4 \times 10^{18}$atm). Both showed signs of surface degradation, with the effect increasing with temperature. In addition, on the 1100°C sample, there was a small buildup of metallic-appearing material on the edge of the wafer closest to the Cr source. Both of these samples, as well as an As-received wafer, have been sent for SIMS analysis of the Cr profile.

In the second experiment, two GaAs wafers were annealed for two hours with a CrAs (powder) source, one at 900°C and the other at 1100°C. The 1100°C sample came out as one large ball of material. The 900°C sample exhibited surface degradation similar to that of the 1100°C sample with the Cr source. This is also being analyzed by SIMS.

6. RAPID REDISTRIBUTION AND GETTERING OF OXYGEN IN CZ-Si

As an adjunct to the present program on impurity motion and gettering in semiconductor materials, we decided to use some of the technology and analytical procedures developed for investigating the problem of oxygen mobility in Si.

The role of oxygen in influencing the electrical properties of silicon has received considerable attention over the past ten years. With the increasing demand for more detailed information on impurity redistribution and process-induced alterations to materials properties, the subject of oxygen redistribution in Si has remained an illusive topic and inferences have typically been drawn from bulk infrared absorption measurements on Si wafers. However, such techniques have limited utility in the investigation of localized redistribution of oxygen within regions of importance to device technology. In this section, we present the results of investigations on the rapid diffusion of oxygen into defect regions produced by mechanical back surface damage techniques and briefly assess the implications for stabilization of gettering during processing.

6.1 GETTERING OF MOBILE OXYGEN AND DEFECT STABILITY WITHIN BACK SURFACE DAMAGE REGIONS IN Si

In recent investigations[16-20] it has been demonstrated that motion of oxygen toward the center of annealed Czochralski (CZ) Si wafers and subsequent precipitation is effective in producing defects that serve as sites for trapping of impurities in _intrinsic_ gettering procedures. Of equal importance, is the influence of oxygen on damage (thermal) stability in _extrinsic_ gettering. In this paper we present data obtained from secondary ion mass spectrometry (SIMS) profiling, transmission electron microscopy (TEM), secondary ion microscopy, and scanning electron microscopy (SEM) measurements on the role of back surface damage regions in gettering of mobile oxygen and the influence of oxygen precipitation on secondary damage nucleation at the wafer backside.

Samples used in this study were n- and p-type, 75 mm diameter, 400μm thick CZ Si wafers of [100] orientation ($\pm 1°$). Oxygen concentrations in the range, 1.0 to 1.2 x 10^{18} cm^{-3}, were determined by Fourier transform infrared (FTIR) absorption measurements on unannealed wafers using ASTM procedures[21]. Back surface damage was introduced in Si wafers using a rotary abrasion technique [22-24] to create concentric spiral grooves extending to an average depth of $\sim$8 to 10μm into the surface. Annealing was done either in a flowing N$_2$ atmosphere or in an oil-free vacuum system at a vacuum level of $\sim$ 10^{-8} Torr. In separate experiments, samples were annealed under the following conditions: a) 600°C, 1 to 24 hours, b) 1050°C, 1 to 15 hours, c) 600°C, 24 hours + 1050°C, 1 to 15 hours and d) 1050°C, 1 to 5 hours + 600°C, 1 to 10 hours.

Specimens for TEM analyses were prepared by a modified jet thinning procedure. Horizontal sections were prepared by

samples were prepared from a series of stacked 800 μm x 3000 μm strips cut along a <110> direction and embedded in epoxy resin (EPON-812). After chemical/mechanical polishing to a thickness of 150 μm, specimens were ion milled in a Commonwealth Scientific instrument.

Secondary ion mass spectrometry was used to obtain oxygen impurity profiles at the back surfaces of the Si. Samples for cross-sectional SIMS imaging[25] were cleaved along a <110> direction, embedded in a low melting point Sn-Bi alloy, and subjected to chemical/mechanical polishing. In all cases, specimens were analyzed in a Cameca IMS-3f microanalyzer using Cs^+ ion bombardment while detecting $^{16}O^-$ and $^{30}Si^-$ secondary ions. The oxygen concentration levels were determined using standards prepared by ion implanting oxygen into CZ-Si. Residual pressure within the sample chamber during SIMS profiling was $\cong 1 \times 10^{-9}$ Torr while sputtering at a rate of 350 $\overset{\circ}{A}$/sec.

Transmission electron microscopic examination showed that the rotary abrasion process produced a laterally discontinuous array of nested dislocations decreasing in density as a function of depth beneath the level of macroscopic damage grooves. Annealing at 600°C for 1 to 24 hours in either vacuum or flowing N_2 produced no significant annihilation of dislocation line structure; however, dark field electron micrographs showed the presence of small (< 250 $\overset{\circ}{A}$ image diameter) microprecipitates within back surface damage regions either pinned along dislocation lines or in adjacent regions, increasing in density as a function of increasing annealing duration. Examination of double annealed (600°, 24 hour + 1050°C, 1-3 hour) samples showed a dramatic increase in dislocation line concentration (Fig. 12a) and a subsequent increase in the effective width of the damage region at the back surface. In addition, we observed the appearance of well

(a)

0.1 μm

SiO$_x$ precipitation

0.1 μm
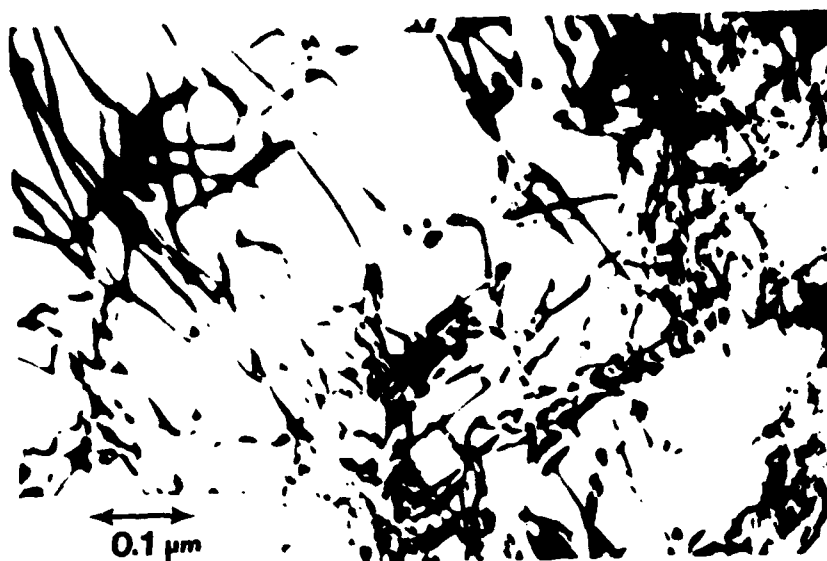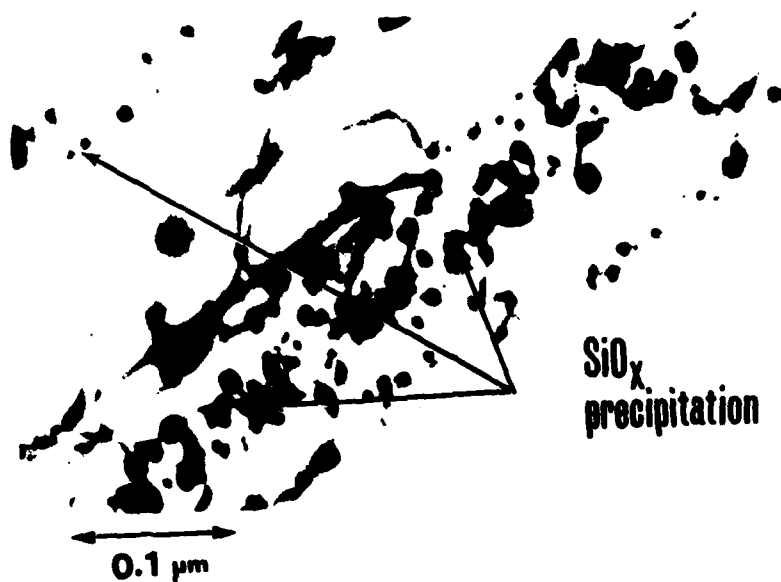
(b)

FIG. 12. BRIGHT-FIELD TRANSMISSION ELECTRON MICROGRAPHS OBTAINED ON BACK-SURFACE DAMAGED SAMPLES SUBJECTED TO VACUUM ANNEALINGS AT 600°C, 24 HRS. + 1050°C. 3 HR: (a) HORIZONTAL SECTION AT DEPTH OF ≈ 5 μ BELOW THE DEPTH OF DAMAGE GROOVES: (b) HIGH MAGNIFICATION MICRO-GRAPH SHOWING THE PRESENCE OF DISLOCATION LINES NUCLEATED WITHIN CLUSTERED SiOx REGIONS. 39

defined SiOx precipitates along dislocation lines and precipitate-dislocation complexes (PDC) associated with the nucleation of clustered precipitates (Fig.(12b)).

Figure 13 shows the measured dislocation line as a function of depth beneath damage grooves. In the damaged control samples and in samples annealed at 600°C for 24 hours, we observed a vertically graded dislocation line structure extending to an estimated depth of $\approx 10 \mu$m. After a double annealing, in either vacuum or flowing N_2, we observed a significant increase in the dislocation line density within the near surface (< 10μm) region and a zone of secondary line structure extending to a depth $\leq 40 \mu$m.

To provide further information on the depth distribution of primary and secondary damage, we prepared vertical cross section samples for TEM analysis. Damaged (unannealed) and 600°C annealed samples contained dislocation lines extending to a depth $\approx 10 \mu$m, in agreement with horizontal sectioning measurements. Examination of double annealed (600°C + 1050°C) samples ({110} surface) showed a heavy concentration of dislocation lines and precipitates within a near surface region (depth $\leq 14 \mu$m) and a secondary zone of dislocation lines extending from the periphery of the region to a depth of $\approx 40 \mu$m. Figure 14 is a representative (vertical cross section) electron micrograph obtained at the edge region of the two zones (d $\sim 14 \mu$m) showing the development of secondary microstructure and precipitation within the primary damage region.

Horizontal sectioning measurements show that $\sim$ 80% of the dislocation line structure is annihilated after a 3-hour, 1050°C anneal. If this high temperature step is followed by 600°C annealing, the development of secondary dislocation line structure (Fig. 14) is not observed.
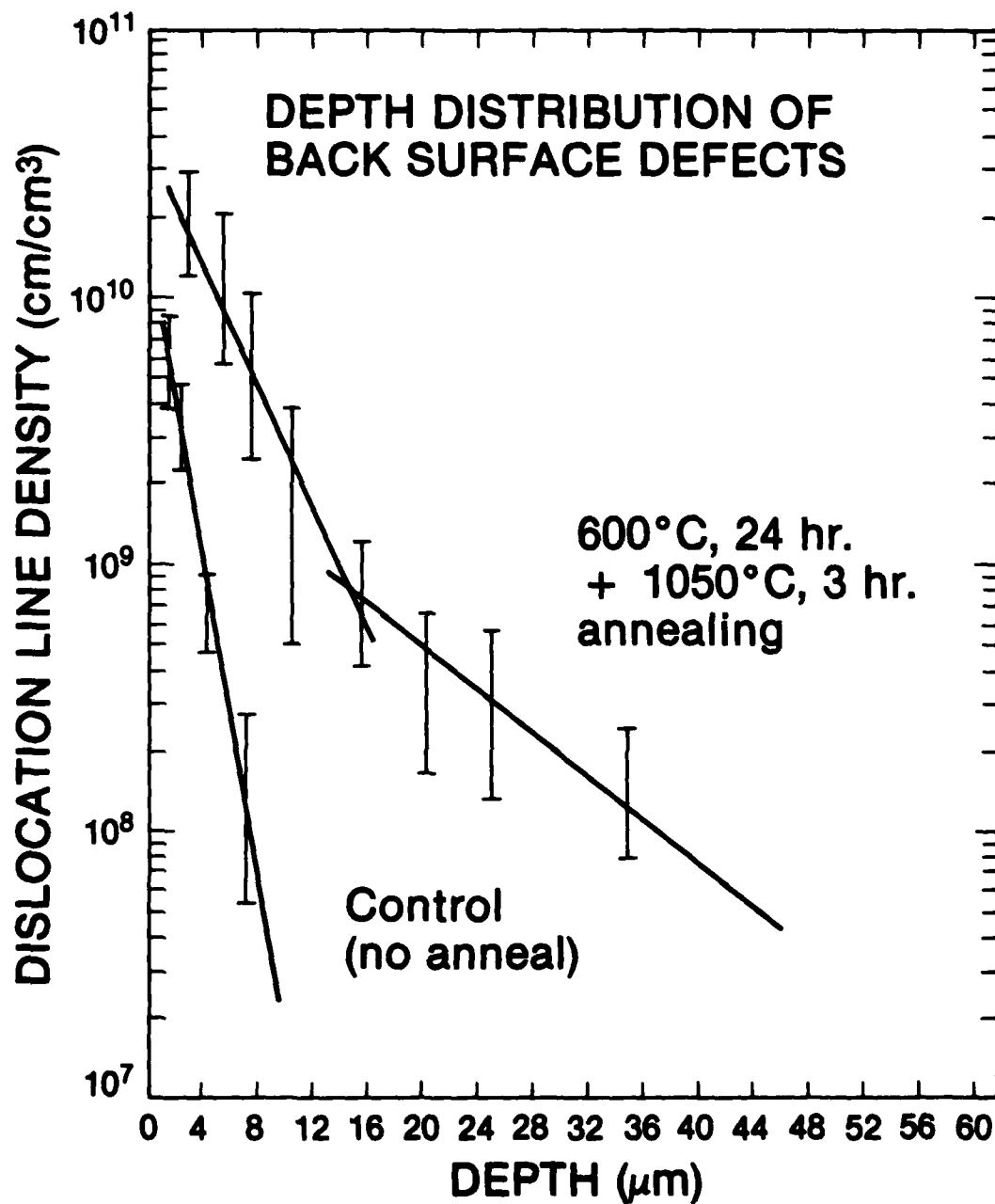
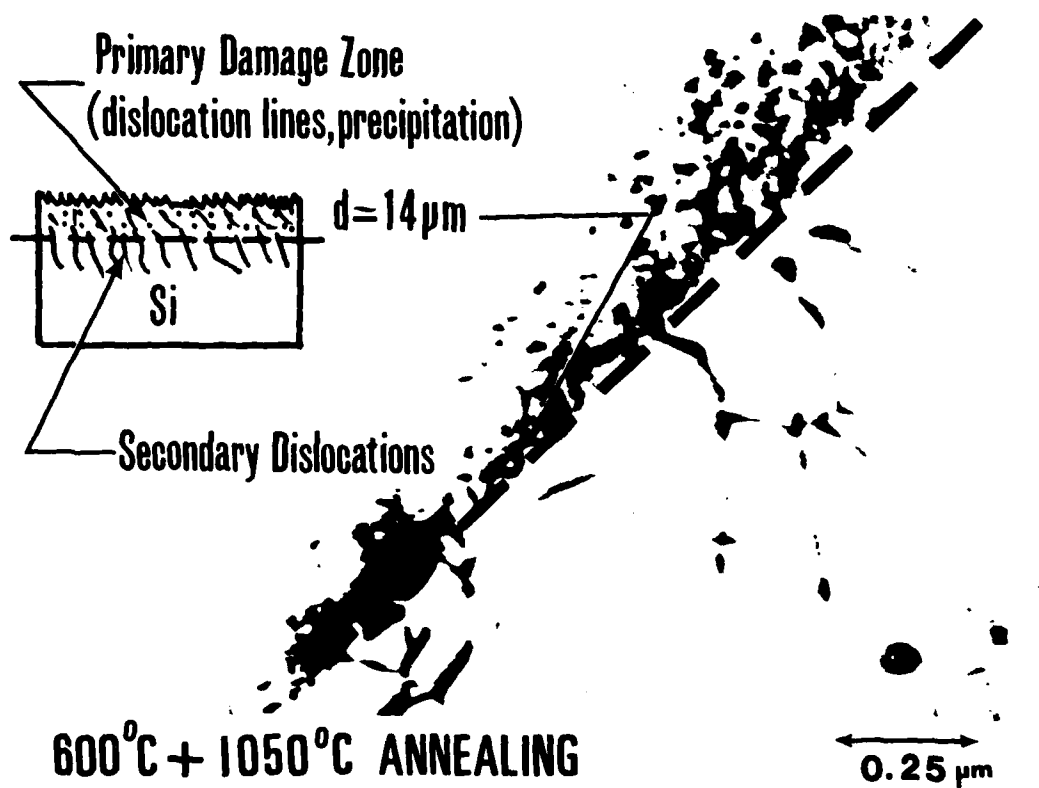FIG. 13. DISLOCATION LINE DENSITY AS A FUNCTION OF DEPTH FOR CONTROL AND DOUBLED-ANNEALED SAMPLES.

41

FIG. 14. BRIGHT-FIELD ELECTRON MICROGRAPHS OBTAINED ON VERTICAL CROSS-SECTION SAMPLES ([100] PLANE) AT DEPTH OF 14 m AFTER ANNEALING AT 600°C FOR 24 HRS. FOLLOWED BY A 3-HRS. ANNEAL AT 1050°C.

A correlation between dislocation line structure and oxygen redistribution was obtained from SIMS profiles of the oxygen concentration beneath damage grooves. Figure 15 shows the SIMS oxygen profiles in control (unannealed) and annealed samples. The control sample shows essentially no redistribution of oxygen, whereas annealing at 1050°C for 1 to 3 hrs. causes oxygen redistribution. Annealing at 600°C for 24 hours produces substantial motion and gettering of oxygen into back surface damage regions. Comparing Figs. 13 and 15 we observe that the oxygen is gettered within a region corresponding to the near surface dislocations. Correspondingly, when the low temperature annealing is followed by a 3 hr., 1050°C annealing treatment, the oxygen profiles again closely parallel the dislocation line density distribution shown in Fig. 13.

Ion micrographs (Fig.16) obtained on vertical cross-sections of annealed samples provide further supportive data on the correlation between oxygen redistribution and damage structure. After annealing at 600°C, dislocation lines are decorated with oxygen atoms and extend to a depth of $\approx 10 \mu$m. After subsequent annealing at 1050°C, the oxygen concentration is dramatically increased within the near surface region, producing a band of precipitated oxygen (Fig. 16b)). Secondary dislocation lines decorated with oxygen extend from the edge of the primary damage zone to a depth of $\approx 40 \mu$m. We detected no internal oxygen banding or secondary damage structure with correlated oxygen precipitation in undamaged or 1050°C annealed samples.

From this data we conclude that annealing of back surface damaged samples at 600°C produces rapid redistribution and gettering of mobile oxygen along dislocation lines. This primary damage is stablized or pinned in the presence of oxygen[26],
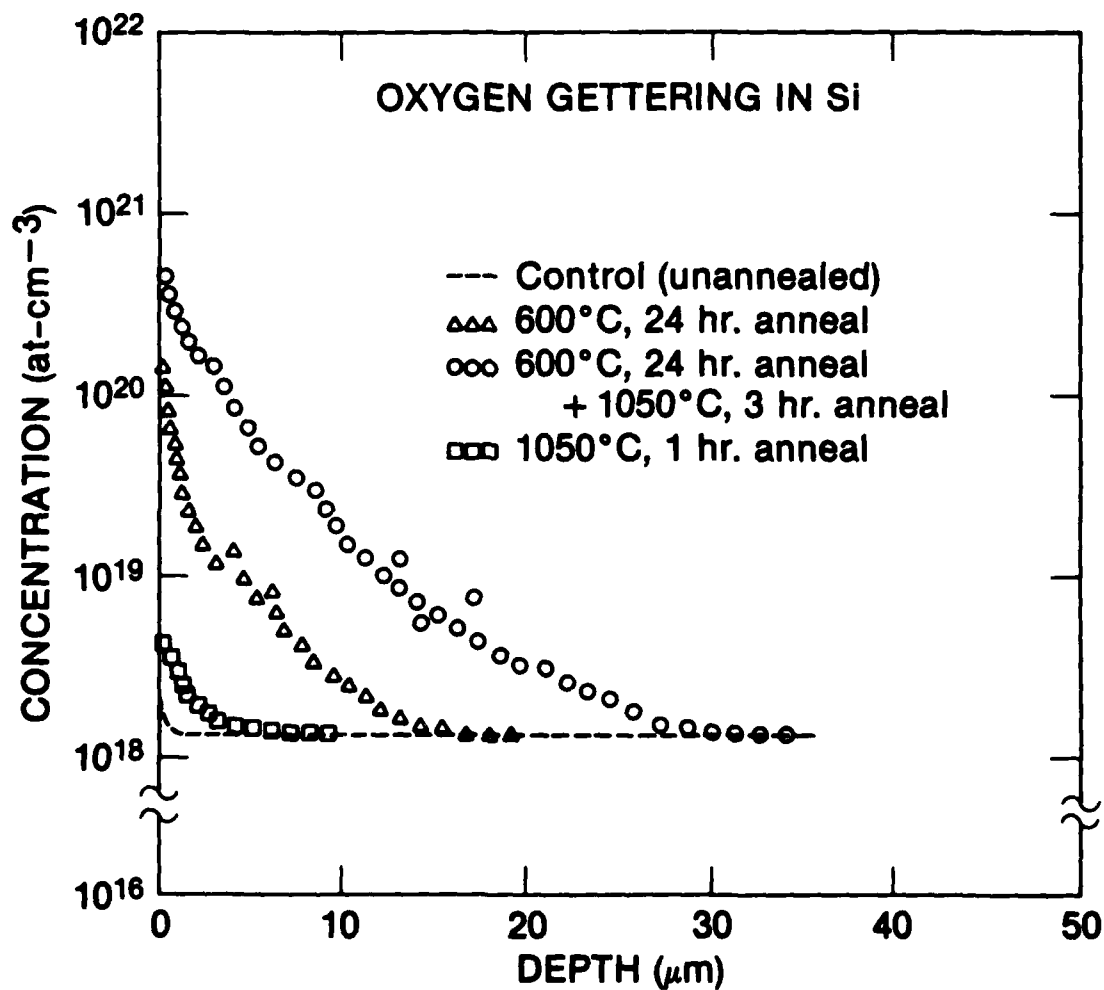
FIG. 15. SIMS PROFILES OF OXYGEN CONCENTRATION AT BACK SURFACE IN
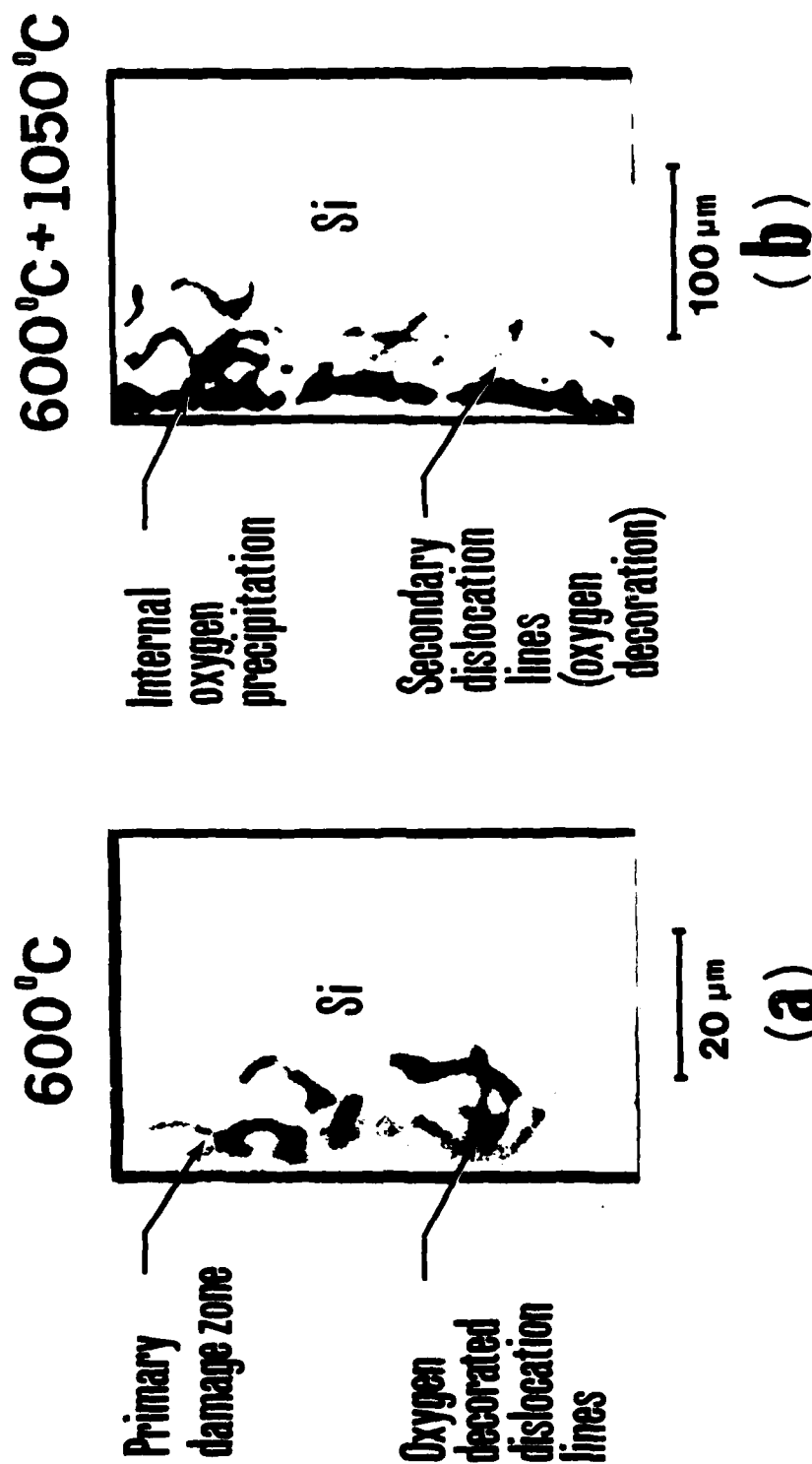DAMAGED, ANNEALED SAMPLES.

44

FIG. 16. SECONDARY-ION MICROGRAPHS SHOWING OXYGEN IMAGES OBTAINED ON [100] PLANES WITHIN BACK-SURFACE DAMAGE REGIONS OF WAFERS SUBJECTED TO ANNEALINGS: (a) 600°C, 24 HRS; (b) 600°C, 24 HR + 1050°C, 3 HR. NEGATIVE PRINTS ARE SHOWN FOR ENHANCED CONTRAST.

with negligible annihilation upon further annealing at 600°C. Subsequent annealing at 1050°C produces additional gettering, oxygen precipitation and an increase in dislocation line density both within PDC clusters and as a result of increased strain fields created by the excessive SiO_x precipitation. Secondary dislocation lines extending to a depth of $\simeq 40 \mu m$ are thought to be generated by large strain fields associated with misfit between SiO_x precipitates and the Si lattice within a heavily precipitated near-surface region. After forming, the secondary dislocation lines serve as sinks for additional gettering of oxygen. Hence, we can conclude that the observed results are related to a rapid diffusion and gettering of mobile oxygen from the bulk background oxygen concentration, with perhaps a small contribution from the surface.

6.2   LOW TEMPERATURE REDISTRIBUTION AND GETTERING OF OXYGEN IN SILICON

To extend the results of the initial investigation on the rapid redistribution of oxygen, a series of experiments were conducted using transmission electron microscopy (TEM), secondary ion mass spectrometry (SIMS) depth profiling and secondary ion microscopy to determine if oxygen can be gettered at temperatures in the range, 300° to 500°C.

Samples for these experiments were n- and p- type, 75 mm diameter, 400 m thick CZ-Si wafers of [100] orientation. Oxygen and carbon concentrations of 1.0 to 1.1 x 10^{18} cm^{-3} and 1.9 x 10^{16}cm^{-3}, respectively, were determined by Fourier transform infrared (FTIR) absorption measurements on unan-

nealed wafers using ASTM procedures[27]. Rotary abrasion techniques[28,29] were used to create concentric grooves of 8 to 10 m depth into the back surfaces of wafers. Annealing was done in either flowing Ar or in an oil-free vacuum system at a pressure of 10^{-8} Torr. Samples were annealed in separate experiments at temperatures between 300° and 500°C for periods of 10 to 72 hours.

Control and annealed samples were prepared for TEM analysis in the form of 3mm x 3mm parallelopipeds. Conventional jet thinning techniques were used to produce electron transparent regions (<3500 Å thick) for examination in the electron microscope. Horizontal sectioning[1] was used to obtain a quantitative measurement of the distribution of microstructural damage as a function of depth at the back surface of damaged wafers.

Oxygen concentrations at the back surfaces of control and damaged, annealed samples were determined using SIMS depth profiling. For cross-sectional analysis, samples were cleaved along a <110> direction, and cut into 1 mm x 5 mm strips. The strips were subsequently stacked and embedded in a low melting point Sn-Bi eutectic alloy. After chemical/mechanical polishing, the specimens were introduced into the chamber of the mass spectrometer and lateral oxygen distributions obtained in the ion imaging mode of operation[25]. All samples were analyzed in a Cameca IMS-3f microanalyzer using Cs^+ primary ion bombardment while detecting $^{16}O^-$ and $^{30}Si^-$ secondary ions. Calibration standards for determining oxygen concentrations were prepared by ion implantation of ^{16}O into CZ-Si.

Examination by TEM of control (undamaged) and back surface damaged (unannealed) samples showed that a later-

ally discontinous complex network of dislocation nests and tangles extending to a depth of $>10 \mu$m was produced by the rotary abrasion process. The dislocation density was observed to decrease as a function of depth, resulting in a vertically graded defect distribution at the back surface of the Si wafer. After annealing at temperatures in the range, 300° to 500°C, for periods of up to 72 hours, we observed no significant alterations in either the lateral or vertical distribution of defects within damaged regions. Careful examination of samples annealed at 300°C for 48 hours showed the presence of small microprecipitates ($\approx$100 to 150Å average image diameter) concentrated at the edges of dislocation lines. Increasing either the annealing time or temperature produced a corresponding increase in the density of microprecipitates, accompanied by only a small increase in average image diameter. In Fig. 17a) we show a representative bright field electron micrograph obtained from the back surface of a sample after annealing at 400°C for 72 hrs. in flowing Ar. The presence of precipitates is clearly noted and observed throughout the damage region. Figure 17b) shows a schematic of the vertical cross section (110 plane) and oxygen ion micrograph obtained from a sample annealed at 400°C for 72 hrs. in flowing Ar. The presence of oxygen along dislocation lines at the back surface is readily observed in the secondary ion micrograph. The majority of oxygen-decorated dislocation line structure is confined to a depth of $\leq$ 10 μm, beneath damage grooves at the back surface, in agreement with horizontal depth sectioning/TEM determinations of dislocation density profiles. In contrast, examination of damaged, unannealed samples in vertical cross section show no oxygen-decorated dislocation line structures by TEM and an apparent absence of any imageable oxygen (by SIMS) within damage regions at the back surface.

0.1 µm

— SiOx Precipitates

(a)

Oxygen gettering region

Oxygen decorated dislocation lines

Back surface

Si {110}

Dislocation lines

10 µm
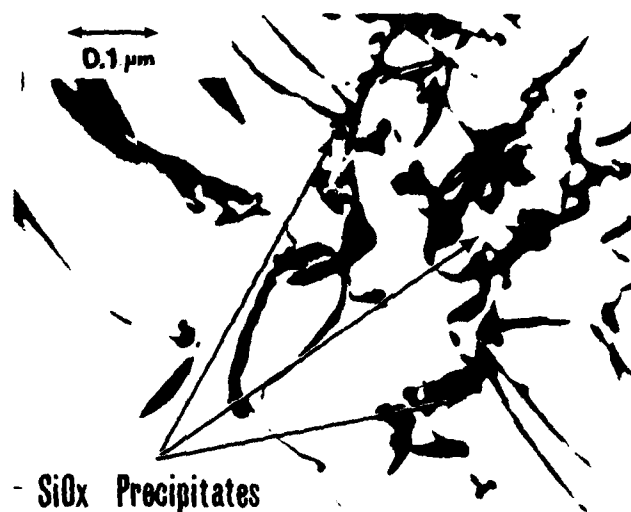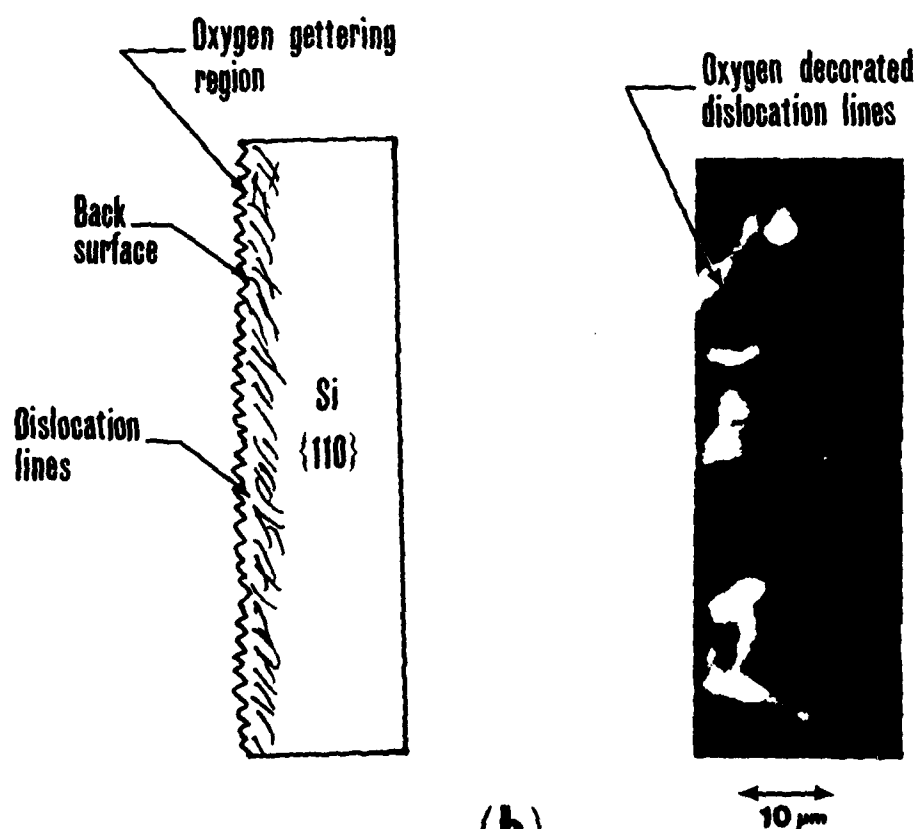
(b)

FIG. 17. BRIGHT-FIELD TRANSMISSION ELECTRON MICROGRAPH AND SECONDARY ION MICRO-GRAPH FROM BACK SURFACE DAMAGED Si SAMPLE AFTER ANNEALING AT 400°C FOR 72 HR; a) BRIGHT-FIELD ELECTROM MICROGRAPH SHOWING THE PRESENCE OF SiOx PRECIPITATES CONCENTRATED ALONG DISLOCATION LINES; b) SECONDARY ION MICRO-GRAPH AND SCHEMATIC SHOWING CROSS SECTIONAL SAMPLE ([100] PLANE) OXYGEN DECORATION ALONG DISLOCATION LINES WITHIN BACK SURFACE DAMAGE REGION.

49

To obtain additonal information on the redistribution of
oxygen as a function of annealing temperature and annealing
time, we obtained SIMS profiles of oxygen concentration as
a function of depth beneath damage grooves at the back sur-
face. Samples were annealed at $300°, 350°, 400°$ and $500°C$ for
periods of 10 to 72 hrs. in separate experiments. For com-
parative purposes we conducted identical annealing experi-
ments in flowing Ar and under high vacuum. Annealing at
$300°C$ for periods <24 hrs. produced no detectable gettering
of oxygen within damage regions. However, for annealing times
>24 hrs. (at $300°C$), we were able to clearly detect the pre-
sence of gettered oxygen at the back surface. Similarly, for
annealing temperatures $>300°C$, the redistribution and gette-
ring of mobile oxygen was noted within damage regions and
observed to increase as a function of increasing annealing
time. Figure 18 shows the relative $^{16}O^-$ion intensity pro-
files obtained at the back surface after damage introduct-
ion (no annealing) and after annealing at variable temper-
atures for 64 and 72 hrs. Also included for reference is
the measured dislocation line density as a function of
depth beneath damage grooves. After annealing at $300°C$ for
64 hrs., oxygen is concentrated within a zone $< 2 \mu$m wide
at the back side of the wafer. When the temperature is in-
creased to $350°C$, the gettered oxygen is distributed over
a region extending 8.0μm below damage grooves at the back
surface. After annealing at $400°C$ or $500°C$ for periods $>$
64 hrs. additional gettering of oxygen is noted throughout
the damage region, resulting in a graded concentration pro-
file that reflects the decreasing dislocation line density
with increasing depth from the back surface. In comparative
tests on vacuum annealed samples and samples annealed in
flowing Ar, no essential difference in the distribution of
gettered oxygen is observed in the profiles obtained, sug-
gesting that the annealing process is not a significant
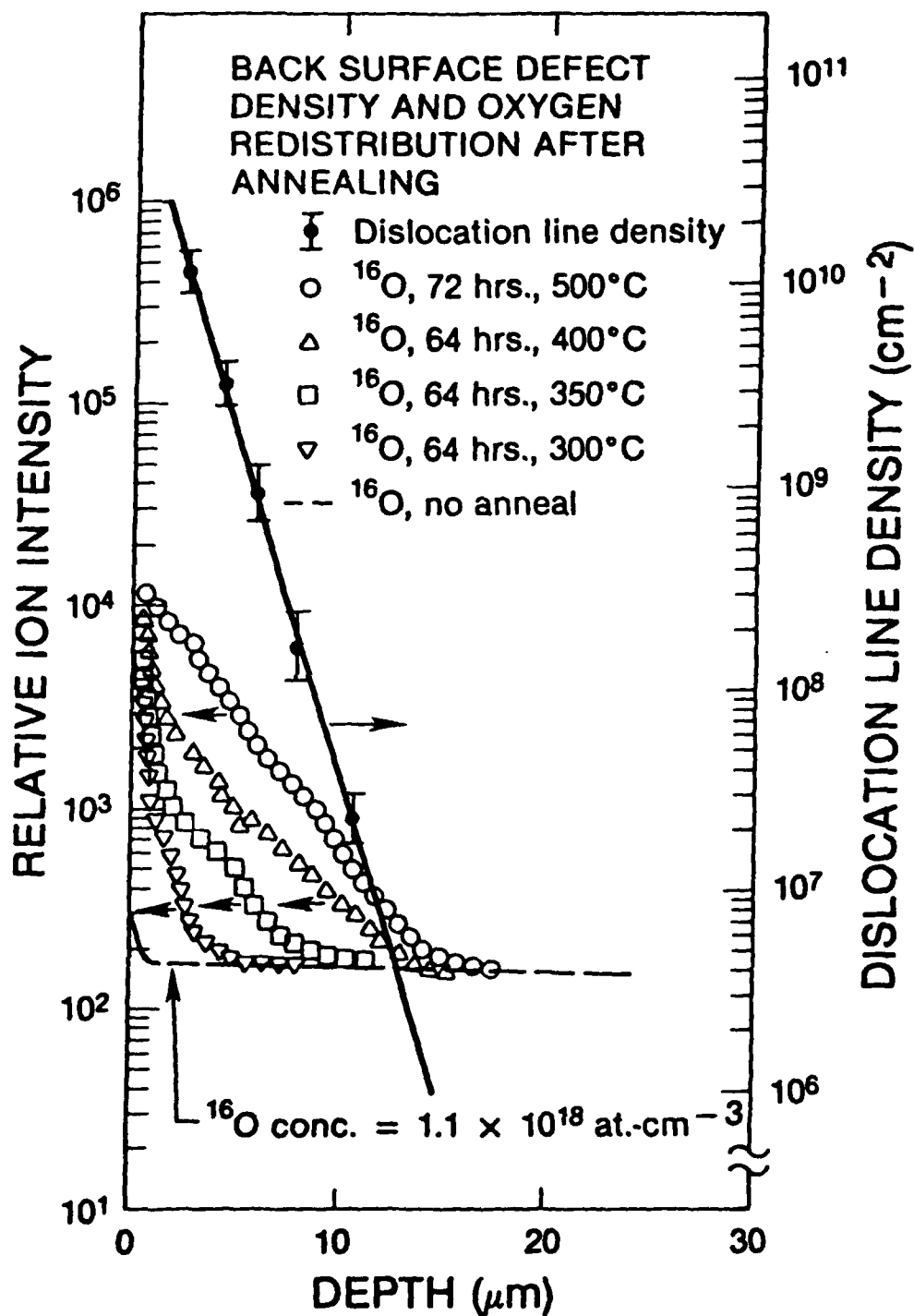oxygen source in these experiments.

FIG. 18. BACK SURFACE DEFECT DENSITY AND SIMS PROFILES OF RELATIVE ^{16}O ION INTENSITIES AFTER ANNEALING AT VARIABLE TEMPERTURES.

Figure 19 shows a semilog plot of the gettered ^{16}O content as a function of $10^3/T(°K)$ for samples annealed for 48 and 72 hrs. at variable temperatures. The amount of gettered oxygen was obtained by integrating the oxygen concentration profiles over the gettering depth, relative to the back surface, with the limit of integration set at the point where the oxygen (gettered) profile intersects the background or bulk oxygen doping level ($1.1 \times 10^{18}/cm^3$). Using the data shown in Fig. 19 an activation energy of 0.92 ± 0.04 eV was computed.

The above data indicate that oxygen is rapidly redistributed and gettered by back surface damage at temperatures as low as 300°C. The process can be characterized by an activation energy of o.92 eV in the presence of a large stress field provided by the vertically graded dislocation line density at the wafer backside. Both transmission electron and secondary ion micrographs confirm the presence of oxygen-related (SiOx) precipitates along dislocation lines. Correlated SIMS profiles also show a graded oxygen profile indicative of the decreasing dislocation line density as a function of depth. From this data we can negate the possibility of enhanced motion of the oxygen via a dislocation line/pipe diffusion mechanism, since transport along a diffusion pipe would not result in a graded oxygen profile. Furthermore, the flux of oxygen atoms moving from the interior of the wafer to the backside would require an additonal driving force for accelerated mass transport.[30] Hence, it appears that the low temperature diffusion and gettering of oxygen observed in these experiments is largely controlled by the magnitude of the stress gradient at the back surface. It can be speculated that similar low temperature diffusion of oxygen will occur in the presence of a stress field, whether such fields are introduced by ion implantation damage, precipitation or contact alloying.
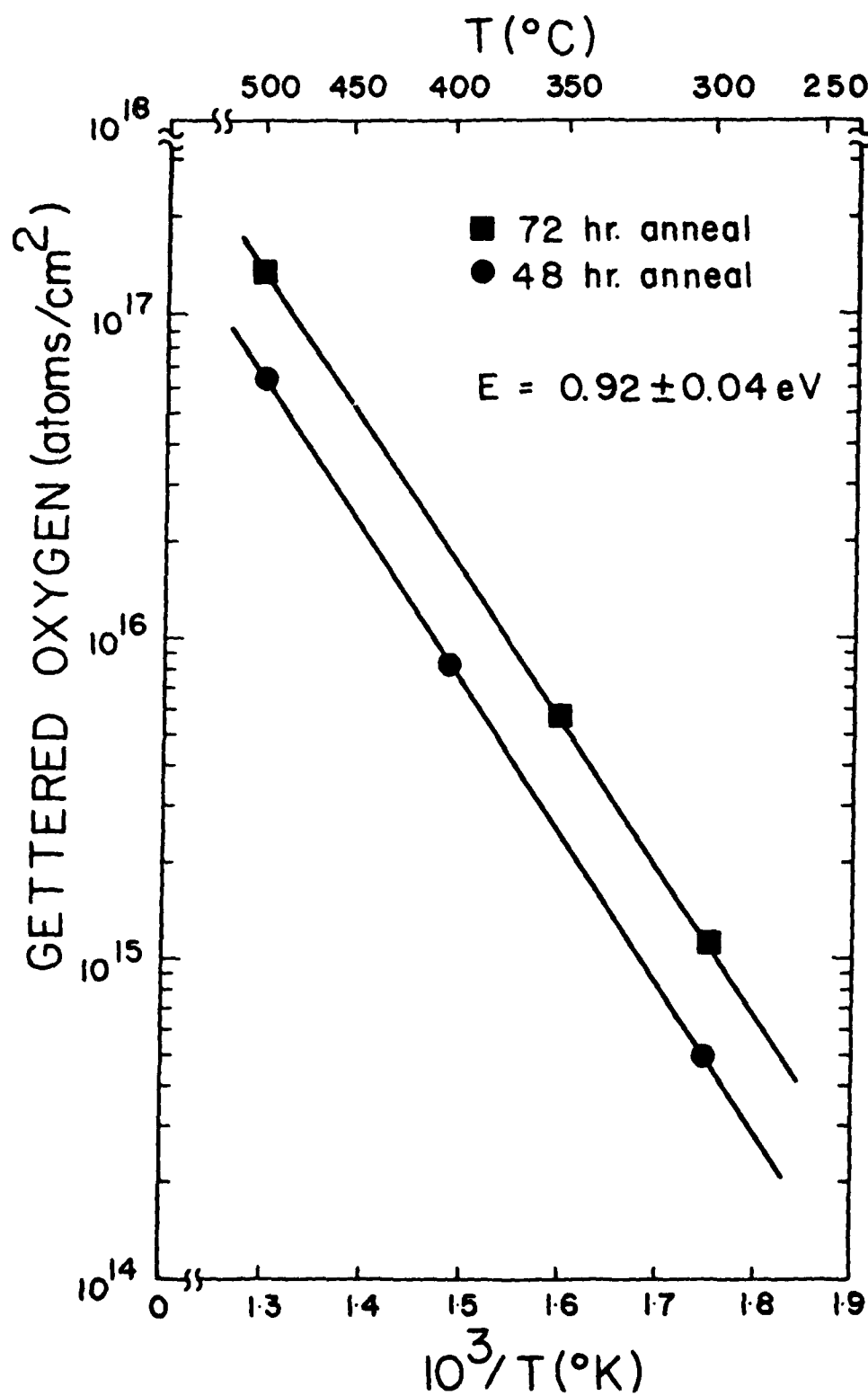
FIG. 19. BACK SURFACE GETTERED ^{16}O CONCENTRATION VS. RECIPROCAL
TEMPERATURE FOR 48- AND 72-HR. ANNEALING PERIODS.

REFERENCES

1. A. M. Huber, G. Morilot, N.T. Linh, P.N. Favennec, B. Deveand and B. Toulouse, Appl. Phys. Lett. 34, 859(1979).

2. C. A. Evans, Jr., V. R. Deline, T. W. Sigmon and A. Lidow, Appl. Phys. Lett. 35, 291(1979).

3. P. N. Favennec and H. L. Haridon, Appl. Phys. Lett. 35, 699(1979).

4. T. J. Magee, J. Peng, J. Hong, C.A. Evans, Jr., V.R. Deline and R. M. Malbon, Appl. Phys. Lett. 35, 277(1979).

5. T.J. Magee, J. Peng, J.D.Hong, V.R. Deline and C.A. Evans,Jr.,Appl. Phys. Lett. 35, 615(1979)6. J. Kasahara

6. J. Kasahara and N. Watanabe, Japanese J. Appl. Phys. 19, L151(1980).

7. P.M. Asbeck, J. Tandon, B.M. Welch, C.A. Evans, Jr., and V.R. Deline, IEEE Electron Device Lett. EDL-1, 35(1980).

8. T. J. Magee, J. Hung, V.R. Deline and C.A. Evans, Jr., Appl. Phys. Lett. 37, 53(1980).

9. T.J. Magee, K.S. Lee, R. Ormond, R.J. Blattner and C.A. Evans, Jr., Appl. Phys. Lett. 37, 447(1980).

10. T.J. Magee, K.S. Lee, R.D. Ormond, C.A. Evans, Jr., R.J. Blattner and C. Hopkins, Appl. Phys. Lett. 37, 635(1980).

11. J. R. Arthur, J. Phys. Chem. Solids 28, 2261(1967).

12. L. J. van der Pauw, Philips Res. Rpts. 13, 1(1958).

13. C. G. Hopkins, V.R. Deline, R.J. Blattner, C.A. Evans,Jr., and T.J. Magee, Appl. Phys. Lett. 36, 989(1980).

14. P. K. Vasudev, R.G. Wilson and C.A.Evans, Jr., Appl. Phys. Lett. 37 308(1980).

15. B. M. Welch, North American Rockwell (private communication), (1980).

16. T. Y. Tan, E. E. Gardner and W. K. Tice, Appl. Phys. Lett. 30, 175(1977).

17. S. Kishino, S. Isomae, M. Tamura and M. Maki, Appl. Phys. Lett. 32, 1(1978).

18. K. Yamamoto, S. Kishino, Y. Mashushita and T. Iizuka, Appl. Phys. Lett. 36, 195(1980).

19. S. Kishino, M. Kanamori,, N. Yoshihiro, M. Tajima and T. Iizuka, Appl. Phys. 50, 8280(1979).

20. F. Shimura, H. Tsuya and T. Kawamura, Appl. Phys. Lett. 37, 483(1980).

21. Annual Book of ASTM Standards (ASTM, Philadelphia, 1977), Pt. 43, F-121.

22. T. J. Magee, J. Peng, J. D. Hong, C. A. Evans, Jr., V. L. Deline and R. M. Malbon, Appl. Phys. Lett. 35, 277(1979).

23. T. J. Magee, J. Peng. J. D. Hong. W. Katz and C. A. Evans, Jr. Phys. Stat. Sol. (A) 55, 161(1979).

24. J. E. Lawrence, Met. Soc. AIME 242 484(1968).

25. G. H. Morrison and G. Slodzian, Anal. Chem. 47, 932A (1975).

26. S. M. Hu, Appl. Phys. Lett. 31, 53(1977).

27 Annual Book of ASTM Standards (ASTM, Philadelphia, 1977, Pt. 43, F-121).

28. J.E. Lawrence, Met. Soc. AIME 242, 484 (1968).

29. T. J. Magee, J. Peng, J. D. Hong, W. Katz and C. A. Evans, Jr., Phys. Stat. Sol. (A) 55, 161 (1979).

30. P.G. Shewman, Diffusion in Solids, (McGraw-Hill, New York, 1971), Chap. 1.

APPENDIX I : TECHNICAL REPORTS PUBLISHED

1. ARACOR Technical Report G-200, "Chromium Depletion Channels and Device Applications," (June, 1980).

2. ARACOR Technical Report G-201, "Field Enhanced Diffusion of Cr in GaAs," (September,1980).

3. ARACOR Technical Report G-202, "Anomalous Diffusion of Oxygen in CZ-Si," (October,1980).

4. ARACOR Technical Report G-203, "Enhanced Diffusion of Cr in InP," (October,1980).

DISTRIBUTION LIST - TECHNICAL REPORTS
Contract No. N00014-80-C-0482

DARPA
1400 Wilson Blvd.
Arlington, VA 22209
(Attn: Program Management) 2

Office of Naval Research 6
Code 427Y
800 North Quincy Street
Arlington, VA 22217

Naval Research Laboratory
4555 Overlook Avenue, S.W.
Washington, D.C. 20375
Attn: Code 2627 6
            6800 1

Office of Naval Research 1
   Branch Office
1030 East Green Street
Pasadena, CA 91101

TACTEC 1
Battelle Memorial Institute
505 King Avenue
Columbus, OH 43201

Defense Contract Administration
   Services 1
Management Area San Francisco
1250 Bayhill Drive
San Bruno, CA 94066

Defense Documentation Center 12
Building 5, Cameron Station
Alexandria, VA 22314

Dr. Y. S. Park
AFAL/DHR
Building 450
Wright-Patterson AFB
Ohio 45433

ERADCOM
DELET-M
Fort Monmouth, NJ 07703

Texas Instruments
M.S. 105/W. Wisseman
P. O. Box 5936
Dallas, TX 75222

Commanding Officer
Office of Naval Research
   Branch Office
1030 East Green Street
Pasadena, CA 91101

Dr. M. Malbon/M.S. 1C
Avantek, Inc.
3175 Bowers Avenue
Santa Clara, CA 94304

Mr. R. Bierig
Raytheon Company
28 Seyon Street
Waltham, MA 02154

Dr. R. Bell, K-101
Varian Associates, Inc.
611 Hansen Way
Palo Alto, CA 94304

Dr. H. C. Nathanson
Westinghouse Research and
   Development Center
Beulah Road
Pittsburgh, PA 15235

Dr. F. Blum/Dr. Daniel Chen
Rockwell International
   Science Center
P. O. Box 1085
Thousand Oaks, CA 91360

Mr. G. J. Gilbert
MSC
100 Schoolhouse Road
Somerset, NJ 08873

Dr. C. Krumn
Hughes Research Laboratory
3011 Malibu Canyon Road
Malibu, CA 90265

Mr. Lothar Wandinger
ECOM/AMSEL/TL/IJ
Fort Monmouth, NJ 07003